Transmission Electron Microscopy

Conventional Imaging

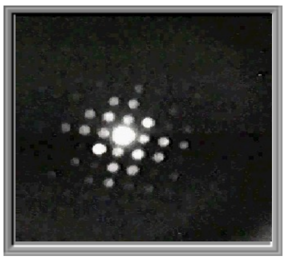

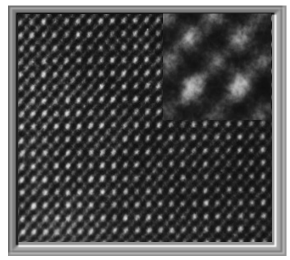

High Resolution Imaging

Diffraction

1

1

A Few References:

Principles and Techniques of Electron Microscopy: Biological Applications
M.A. Hayat CRC Press 1989

Electron Microscopy of Thin Crystals
Hirsch, Howie, Nicholson, Pashley, Whelan Kreiger Press 1977

Electron Diffraction Techniques Vols 1 & 2, IUCr Monographs
Cowley ed., Oxford Press 1992

Defect Analysis in Electron Microscopy
Loretto & Smallman , Halsted Press 1975

Transmission Electron Microscopy
Reimer Springer-Verlag 1989

Transmission Electron Microscopy A textbook for Materials Science
Williams & Carter Plenum Press 1996

Introduction to Analytical Electron Microscopy
Hren, Goldstein, Joy Plenum Press 1979

2

2

2

Amplitude/Diffraction vs Phase Contrast Imaging

Conventional TEM vs High Resolution TEM

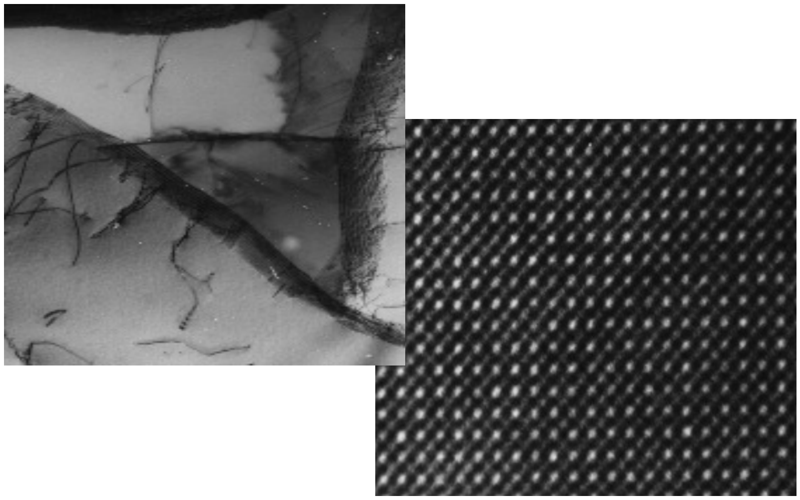

Roles of the Lenses

Gun Lens

Helps form probe

Condenser Lens

Mainly controls:
Spot Size
hence total beam current

Objective Lens

Mainly controls
Focus, 1st Magnification

Diffraction/Intermediate Lens

Controls Mode

Projector Lens

Magnification

Most TEM/STEM have 7-9 Lenses

1 Gun Lens
2-3 Condensers
1 Objective
1-2 Intermediate
1-2 Projectors

Most instruments Have Electromagnetic Round Lenses

Exception:
Aberration Corrected Systems

Note the locations of the various Apertures.

Optimum aperture sizes are needed for various imaging functions.

CTEM Image generally with underfocused/parallel Illumination

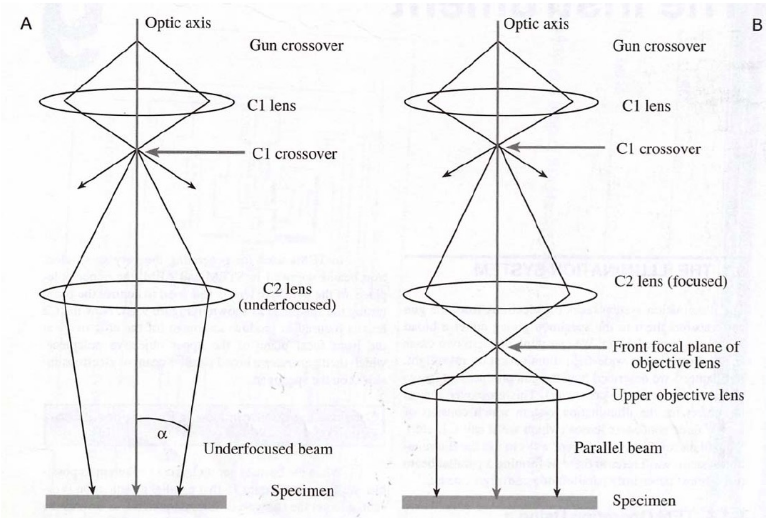

Figure 9.1. Parallel-beam operation in the TEM (A) using just the C1 and an underfocused C2 lens and (B) using the C1 and C2 lenses to image the source at the front focal plane of the upper objective lens.

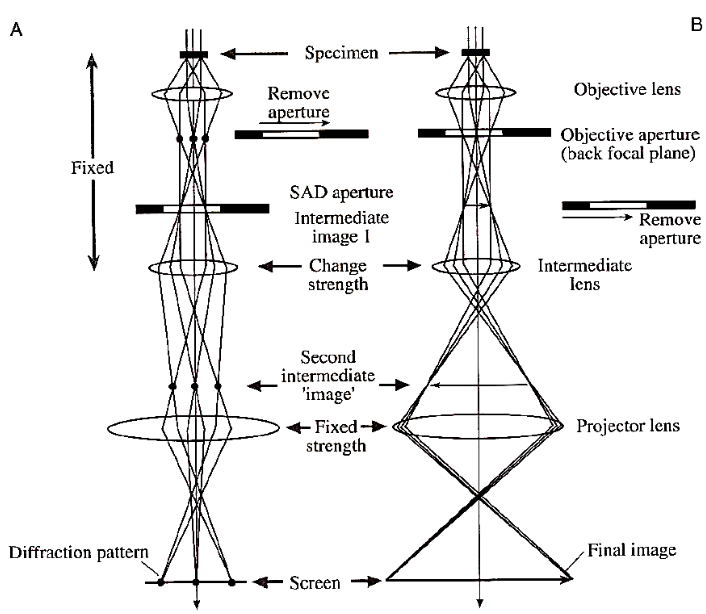

Major Factors affecting TEM Image Contrast

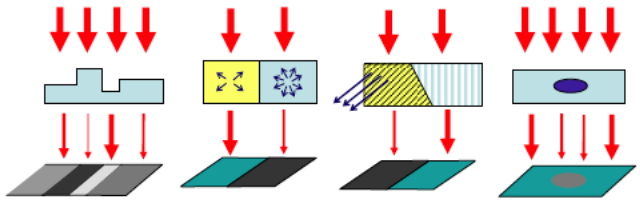

Thickness	Atomic number	Orientation	Defects
Scattering	*Scattering*	*Diffraction*	*Scattering & diffraction*

Contrast Mechanisms

Elastic
- Amplitude (Mass/Thickness) Contrast
  - Varying mass of the specimen attenuates the beam
- Diffraction Contrast
  - Scattered beams are removed or signal from scattered events is used
- Phase (Interference) Contrast
  - Scattered beams constructively or destructively intereact with each other

Inelastic
  - Signal derived from probe changing energy/momentum in the specimen

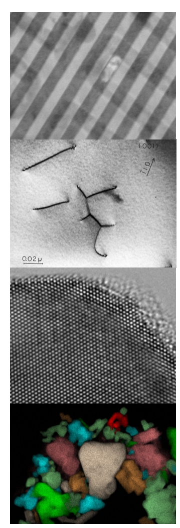

Contrast in the TEM

- Mass contrast
  - Varying mass of sample attenuates the beam differently.
- Diffraction contrast
  - Bragg scattered beams are removed.
- Phase contrast
  - Bragg scattered beams interfere with each other.

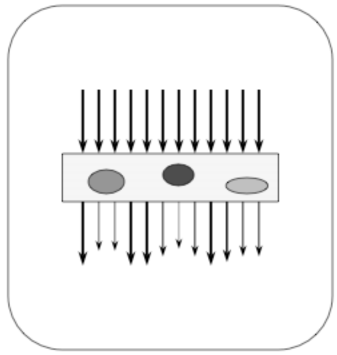

9

9

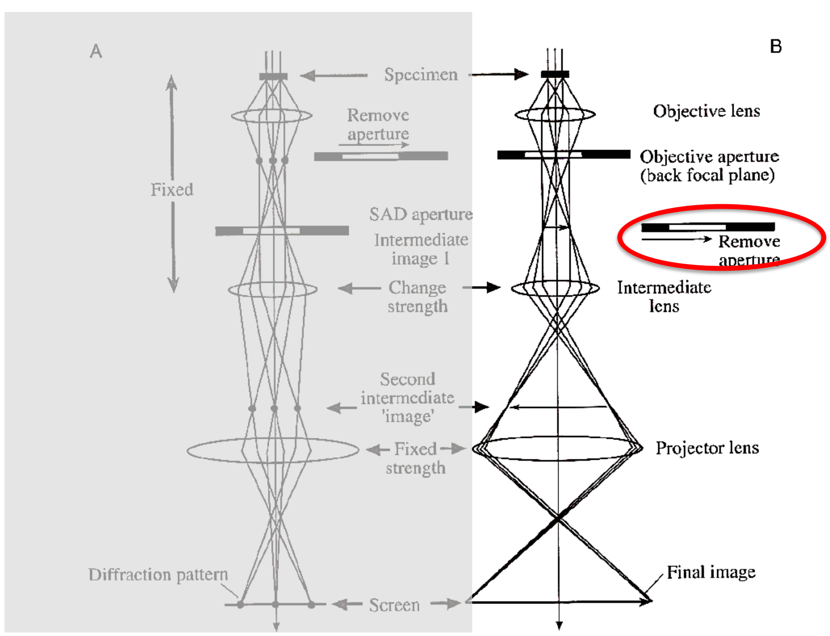

10

10

Zaluzec - 2023

Elastic Scattered Intensity

Amorphous Solids:

$$I(\theta) \sim |f(\theta)|^2 \bullet \left\{1 + \frac{\sin(kR)}{kR}\right\}$$

$$k = \frac{4\pi}{\lambda}\sin(\theta)$$

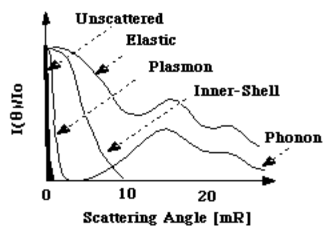

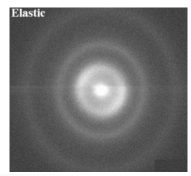

11

11

Zaluzec - 2023

Mass-Thickness Contrast

- This is the most important type of contrast for biological specimen imaging. In particular, for imaging non-crystalline materials such as tissues, cells, and polymers.
- It is expected that high-Z (i.e., high-mass) regions of a specimen scatter more electrons than low-Z regions of the same thickness.
- Similarly, thicker regions will scatter more electrons than thinner regions of the same average Z, all other factors being constant.
- Therefore, for the case of a BF image, thicker and/or higher-mass areas will appear darker than thinner and/or lower-mass areas. The reverse will be true for DF image.

12

12

Amplitude Contrast

$$\nabla^2\Psi + \frac{8\pi^2 m}{h^2}(E+V_0)\Psi = 0$$

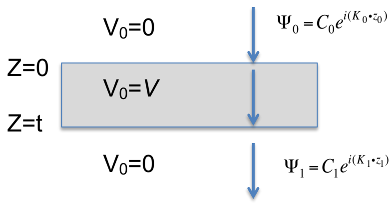

$$\boxed{I = |\Psi_1 \Psi_1^*| = I_0 \mathrm{e}^{-Qt}}$$

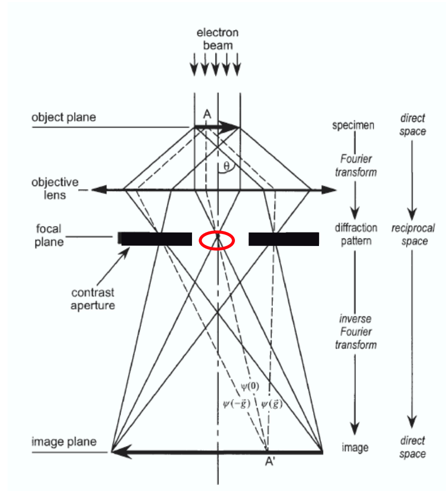

Amplitude Contrast to a first approximation images the "unscattered" beam
An aperture is used to permit only the directly transmitted beam

Amplitude Contrast : Stained Biological Tissue

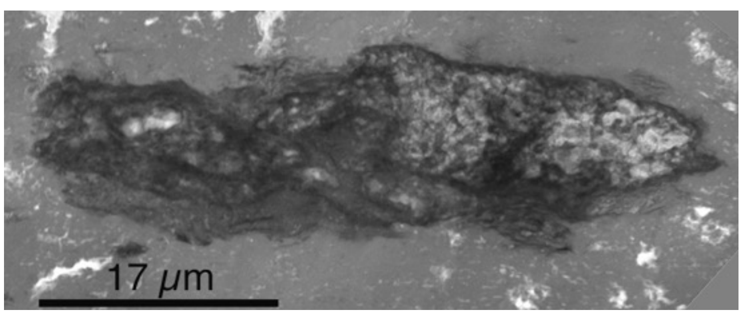

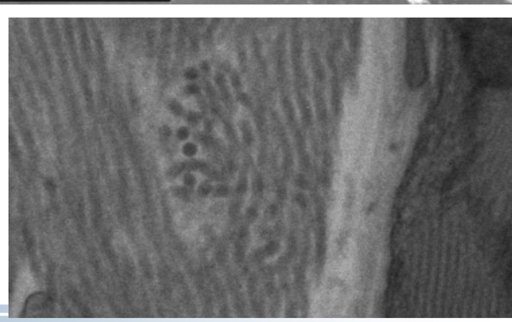

Electromigration Voids in "Real Devices"

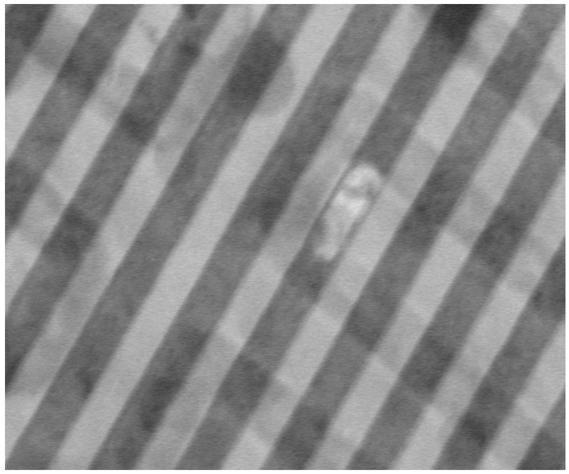

Amplitude contrast Thick Material

Zaluzec - 2023

Phase Contrast

$$\nabla^2\Psi + \frac{8\pi^2 m}{h^2}(E+V_0)\Psi = 0$$

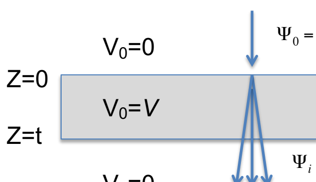

$$\Psi_0 = C_0 e^{i(K_0 \cdot z_0)}$$

$$\Psi_i = C_i e^{i(K_i \cdot z_i)}$$

$$\Psi_T = \sum \Psi_i$$

$$\boxed{I = |\Psi_T \Psi_T^*| = I_0(1 + \mathrm{e}^{-Qt} + ...)}$$

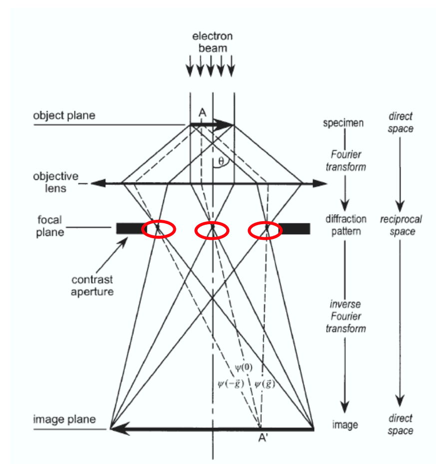

Phase Contrast results from interference between multiple waves
Large or No apertures used – allows many beams to interact.

Non-crystalline samples
Amplitude vs Phase
Thin Samples

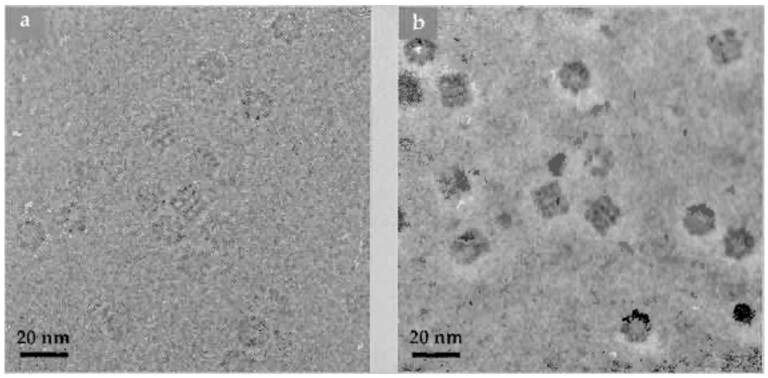

Mainly Amplitude Contrast

Contrast Enhanced
With Phase Contrast

17

17

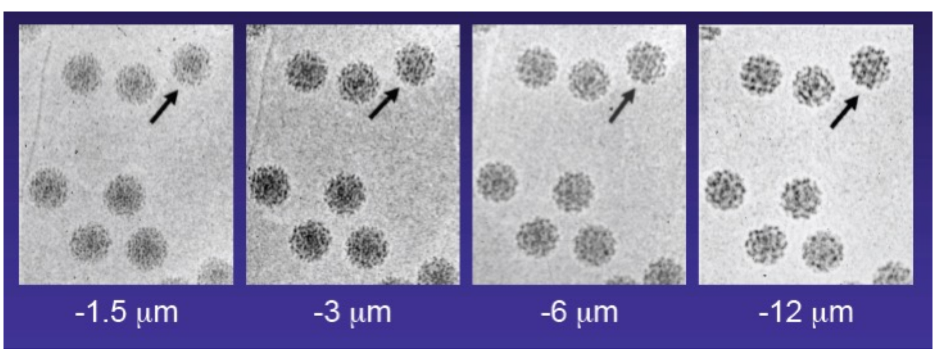

Phase Contrast is Increased by defocusing
But the "image resolution" degrades due to Fresnel Diffraction

18

18

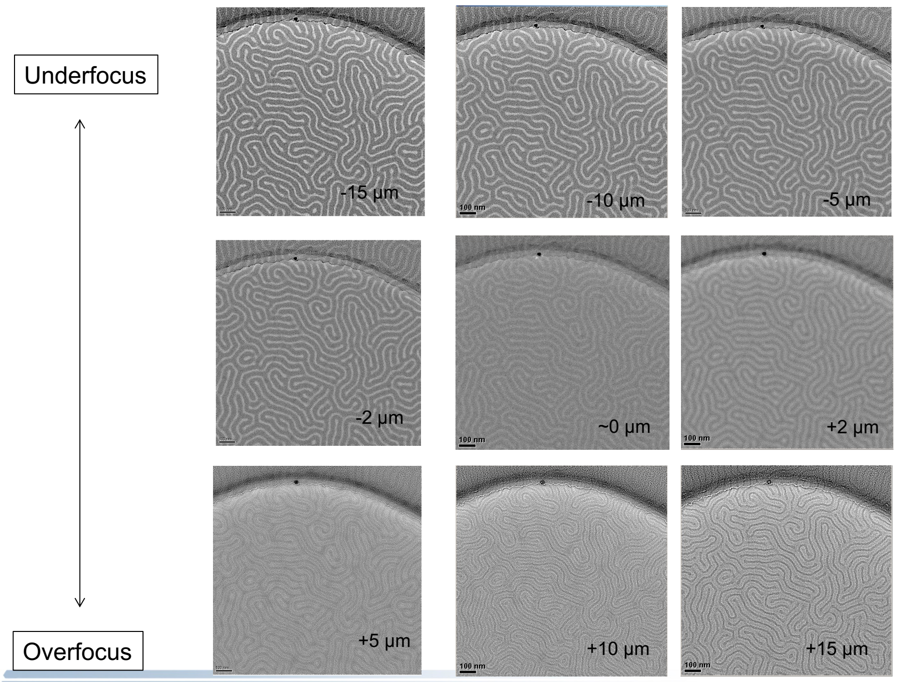

19

Diffraction Contrast

Elastic Scattering

Crystalline Solids:

$$I(\theta) \sim |F(hkl)|^2$$

$$F(hkl) = \sum_j f_j(\theta)\ e^{(-2\pi i \vec{k}\cdot\vec{r})}$$

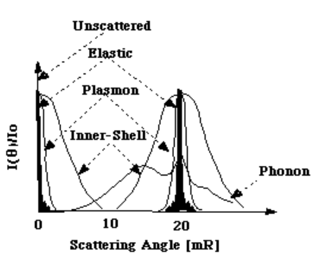

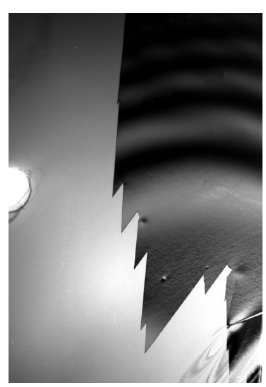

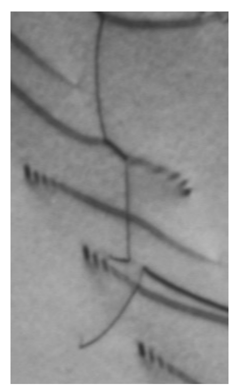

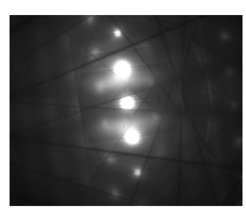

20

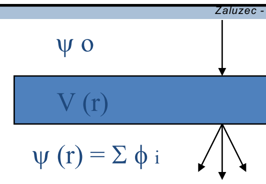

TEM/HREM Image Interpretation/Calculation
(well beyond a 60 minute lecture)

$$\nabla^2\psi(\mathbf{r}) + (8\pi^2 me/h^2)[E + V(\mathbf{r})]\psi(\mathbf{r}) = 0$$

$$\psi(\mathbf{r}) = \exp\,(2\pi i\boldsymbol{\chi}\,.\,\mathbf{r})$$

$$V(\mathbf{r}) = \frac{h^2}{2me}\sum_g U_g \exp\,(2\pi i\mathbf{g}\,.\,\mathbf{r}) = \sum_g V_g \exp\,(2\pi i\mathbf{g}\,.\,\mathbf{r})$$

$$\psi(\mathbf{r}) = \phi_o(z)\exp\,(2\pi i\mathbf{K}\,.\,\mathbf{r}) + \phi_g(z)\exp\,(2\pi i(\mathbf{K}+\mathbf{g})\,.\,\mathbf{r})$$

$$K^2 = \frac{2meE}{h^2} + U_0 = \chi^2 + U_0$$

$$I = |\psi\psi^*|$$

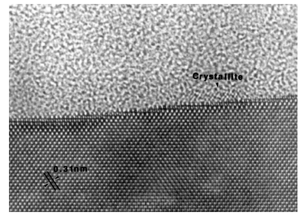

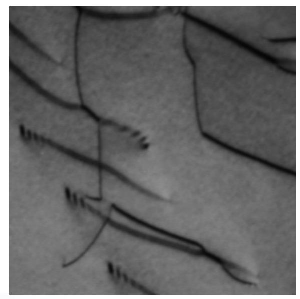

21

21

Zaluzec - 2023

Bright Field

Dark Field

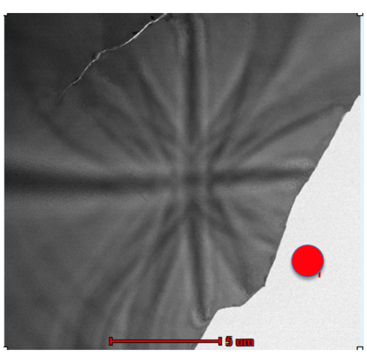

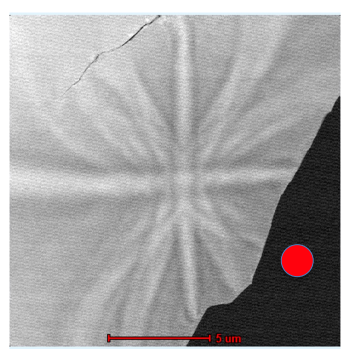

22

22

Bright-Field and Dark-Field Imaging

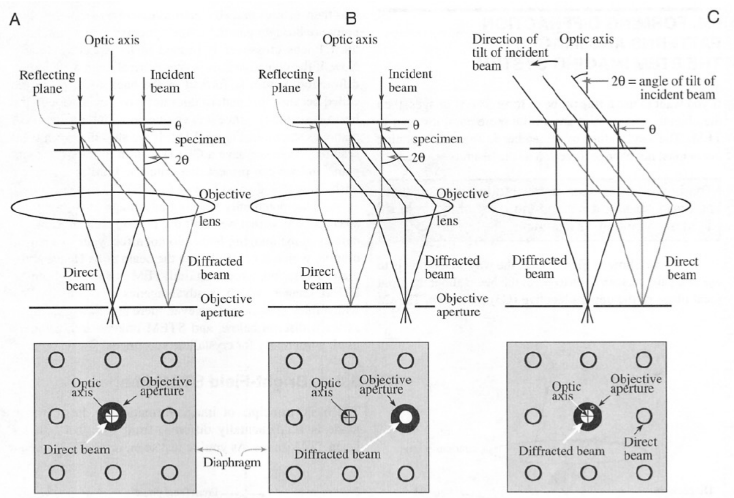

Figure 9.14. Ray diagrams showing how the objective lens/aperture are used in combination to produce (A) a BF image formed from the direct beam, (B) a displaced-aperture DF image formed with a specific off-axis scattered beam, and (C) a CDF image where the incident beam is tilted so that the scattered beam remains on axis. The area selected by the objective aperture, as seen on the viewing screen, is shown below each ray diagram.

Bright Field/Dark Field Imaging

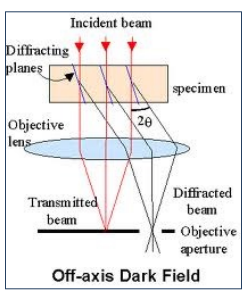

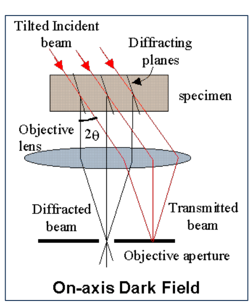

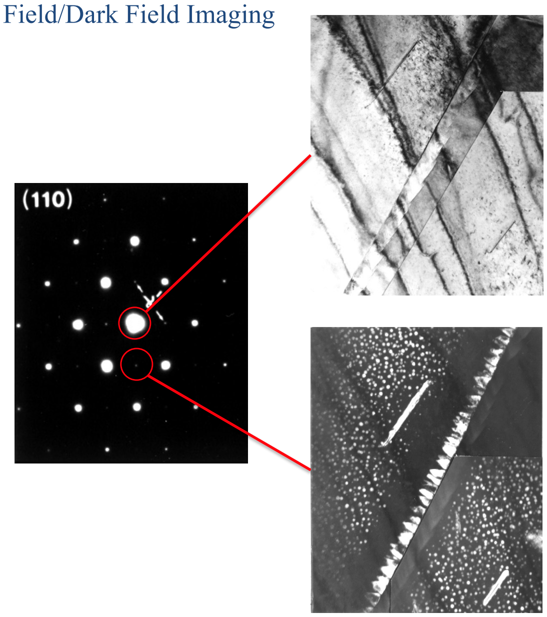

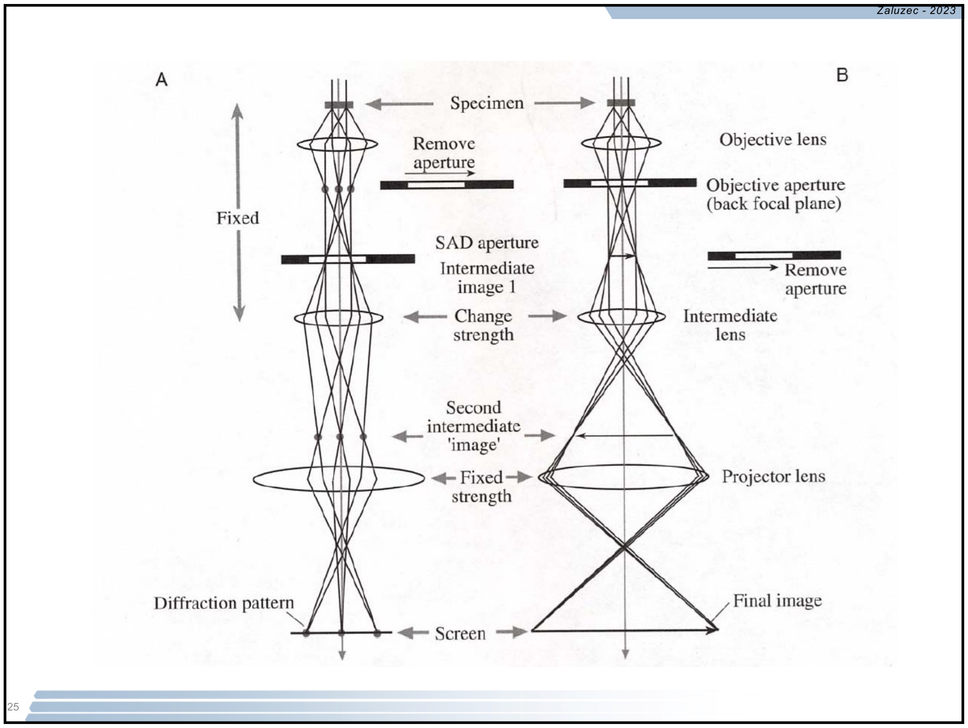
Zaluzec - 2023
A
B
Specimen
Remove aperture
Objective lens
Objective aperture (back focal plane)
Fixed
SAD aperture
Intermediate image 1
Remove aperture
Change strength
Intermediate lens
Second intermediate 'image'
Fixed strength
Projector lens
Diffraction pattern
Final image
Screen
25

25

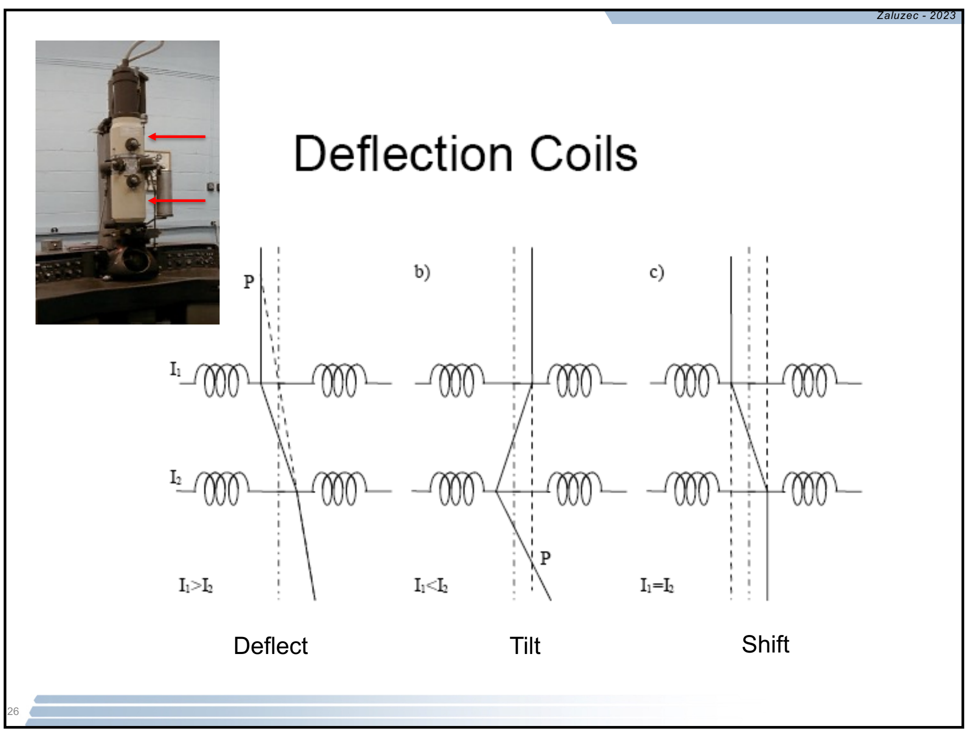
Zaluzec - 2023
Deflection Coils
P
I_1
I_2
$I_1>I_2$
b)
P
$I_1<I_2$
c)
$I_1=I_2$
Deflect
Tilt
Shift
26

26

Bright Field/Dark Field Imaging

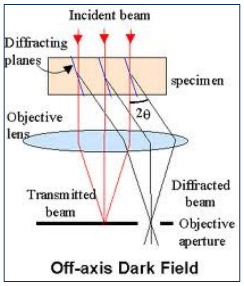

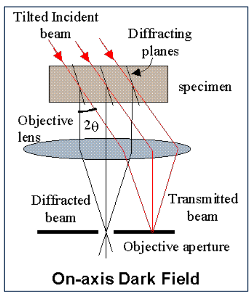

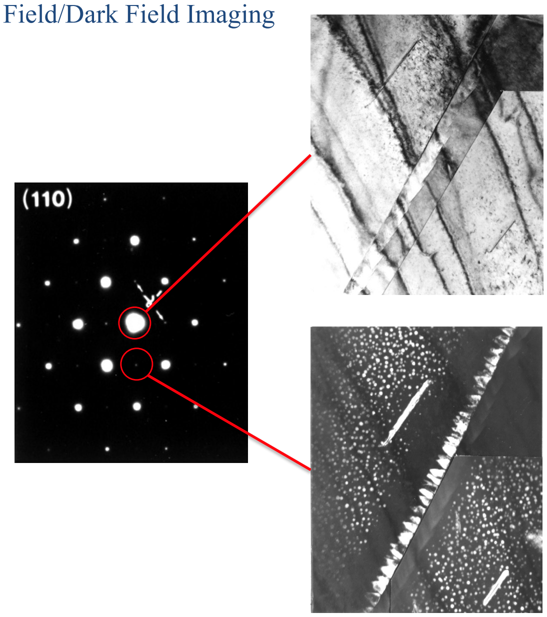

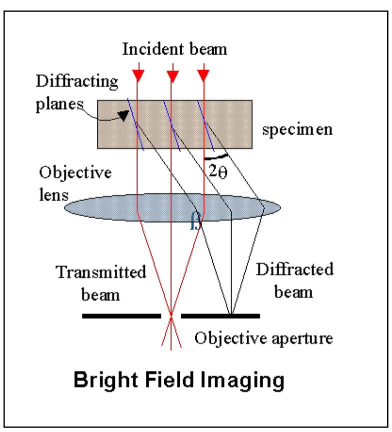

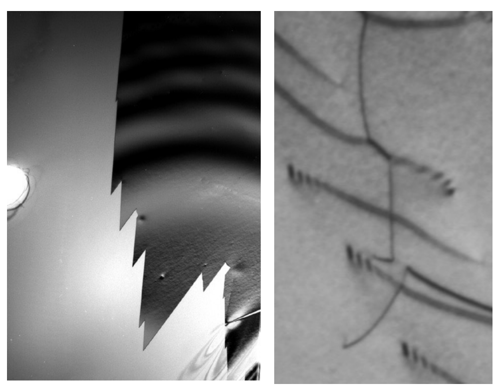

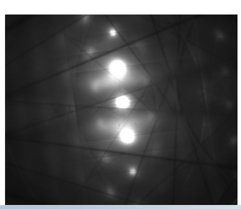

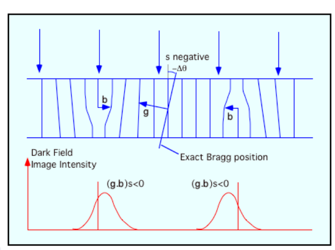

Common Diffraction Contrast Phenomena In Crystalline Materials

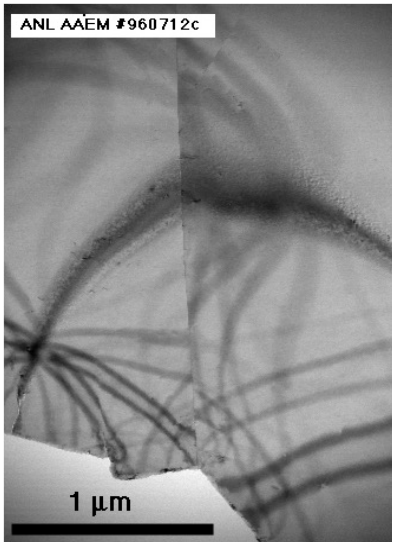

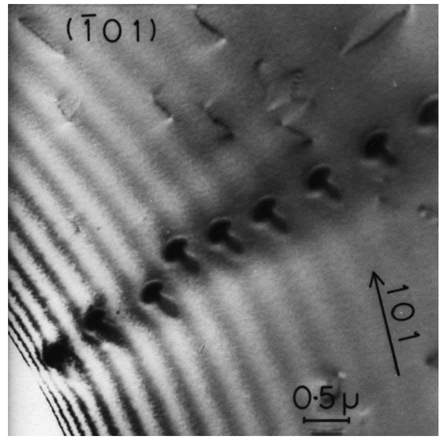

Kinematical Theory of Image (Diffraction) Contrast

1.) Amplitude Contrast
2.) Diffraction into a Beam is small
3.) Multiple Diffraction Events do not occur
4.) Each point of the specimen can be considered independent
of its neigbors (column approximation)
5.) Each slab in the column can be assumed to act as a Fresnel Zone

$$\phi_0 = 1 - \phi_g$$

$$\phi_g = \left(\frac{\pi i}{\xi_g}\right)\int_0^t e^{-2\pi i s_g z}\,dz = \frac{\pi i}{\xi_g}\left(\frac{\sin \pi t s_g}{\pi s_g}\right)\left\{e^{-i\pi t s_g}\right\}$$

$$\xi_g = \pi V_c \frac{\cos(\theta)}{\lambda F(\theta)} \quad \Rightarrow f(Z, E_o, a_i)$$

$$I_g = \phi_g \phi_g^* = \left(\frac{\pi}{\xi_g}\right)^2 \left(\frac{\sin \pi t s_g}{\pi s_g}\right)^2$$

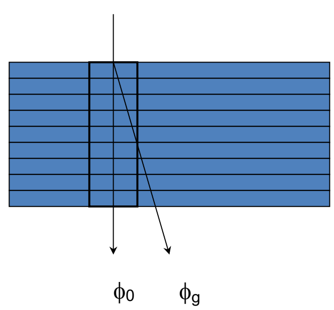

Contrast Variation with Thickness

$$I_g = \phi_g \phi_g^* = \left(\frac{\pi}{\xi_g}\right)^2 \left(\frac{\sin \pi t s_g}{\pi s_g}\right)^2$$

$$s_g = \frac{\sqrt{w^2+1}}{\xi_g}$$

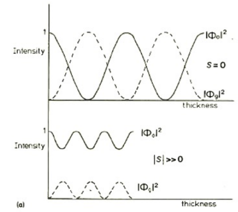

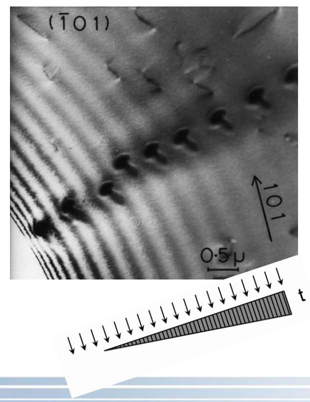

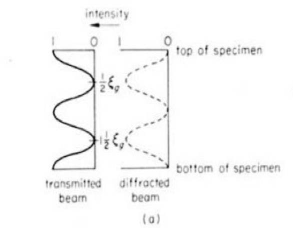

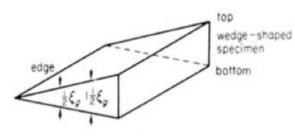

$$I_0 = 1 - I_g$$

$$I_g = |\phi_g|^2 = \left(\frac{\pi}{\xi_g}\right)^2 \frac{\sin^2(\pi t s^{eff})}{(\pi t s^{eff})^2}$$

$$s^{eff} = \sqrt{s^2 + \frac{1}{\xi_g^2}}$$

$$\xi_g^{eff} = \frac{\xi_g}{\sqrt{1+s^2\xi_g^2}}$$

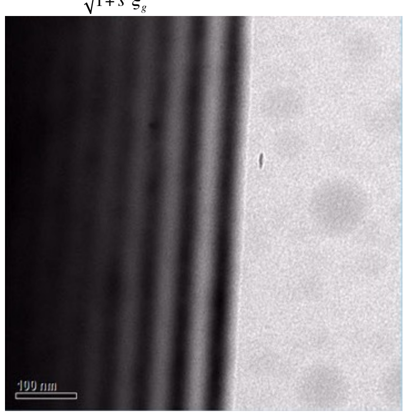

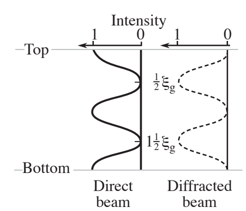

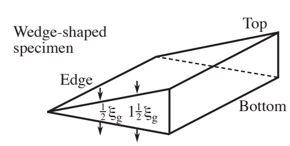

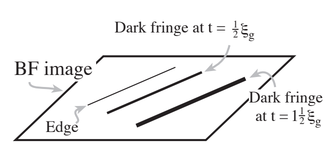

Typical Extinction Distances (nm) @ 100 kV

fcc

Reflection	Al	Cu	Ni	Au	Si	Ge
111	56	24	24	16	60	43
200	67	28	28	18	-	-
220	106	42	41	25	76	45
311	130	51	50	29	135	76
222	138	54	53	31	-	-
400	167	65	65	36	127	66

bcc

Reflection	Fe	Nb	Mo
110	27	26	23
200	39	37	32
211	50	46	41
310	71	62	58

$$\xi_g = \pi V_c \frac{\cos\theta}{\lambda F(\theta)}$$

hcp

Reflection	Mg	Co	Zn	Zr	Cd
0002	81	25	26	32	24
1-101	100	31	35	38	32
11-20	141	43	50	49	44
1-100	151	47	55	59	52
11-22	171	52	58	59	68
2-201	202	62	70	69	61

Contrast Variation with Orientation

$$I_0 = 1 - I_g$$

$$I_g = \phi_g \phi_g^* = \left(\frac{\pi}{\xi_g}\right)^2 \left(\frac{\sin \pi t s_g}{\pi s_g}\right)^2$$

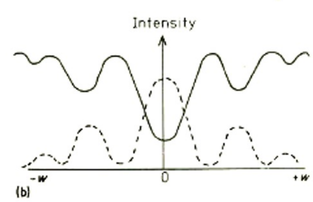

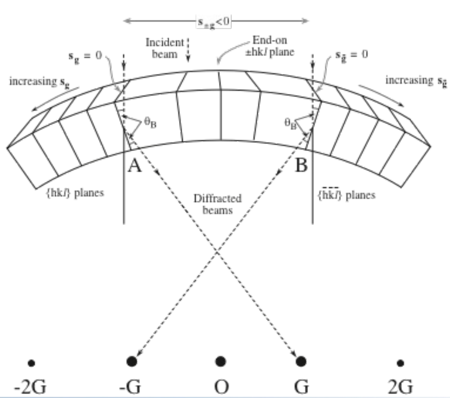

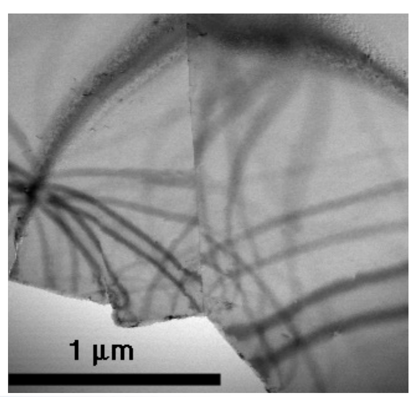

Bend Contours

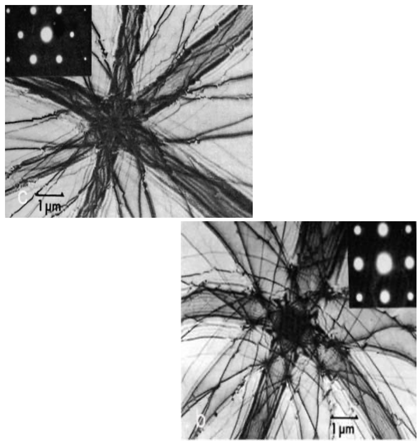

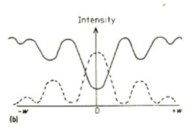

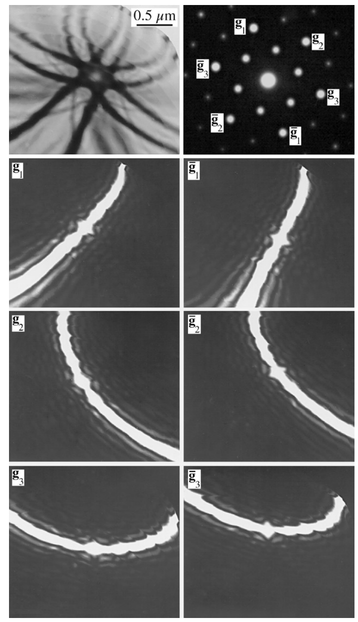

Dynamical Theory of Image Contrast

$$\frac{d\phi_0}{dz} = \left[\frac{\pi i}{\xi_0}\right]\phi_0 + \left[\frac{\pi i}{\xi_g} e^{2\pi i s z}\right]\phi_g$$

$$\frac{d\phi_g}{dz} = \left[\frac{\pi i}{\xi_0}\right]\phi_g + \left[\frac{\pi i}{\xi_g} e^{-2\pi i s z}\right]\phi_0$$

$$I_g = \left|\phi_g\right|^2 = \left(\frac{\pi}{\xi_g}\right)^2 \frac{\sin^2\left(\pi t s_g\right)}{\left(\pi s^{eff}\right)^2}$$

$$s_g = s^{eff} = \sqrt{\frac{w^2+1}{\xi_g^2}} = \sqrt{s^2 + \frac{1}{\xi_g^2}}$$

$$\xi_g^{eff} = \frac{\xi_g}{\sqrt{1+s^2\xi_g^2}}$$

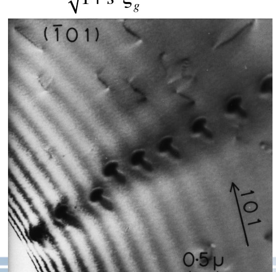

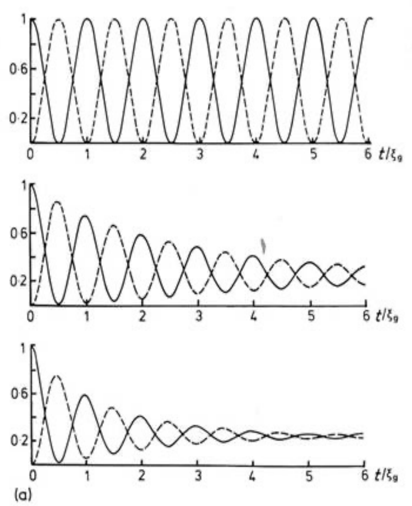

Theoretical profiles of thickness fringes calculated for various values of absorption for a foil of thickness $6\xi_g$. (i) No absorption. (ii) $\xi_g/\xi_g' = 0.05$ (iii) $\xi_g/\xi_g' = 0.10$. Bright and dark field images are indicated by the continuous and dashed lines respectively. (After Hashimoto, Howie and Whelan).

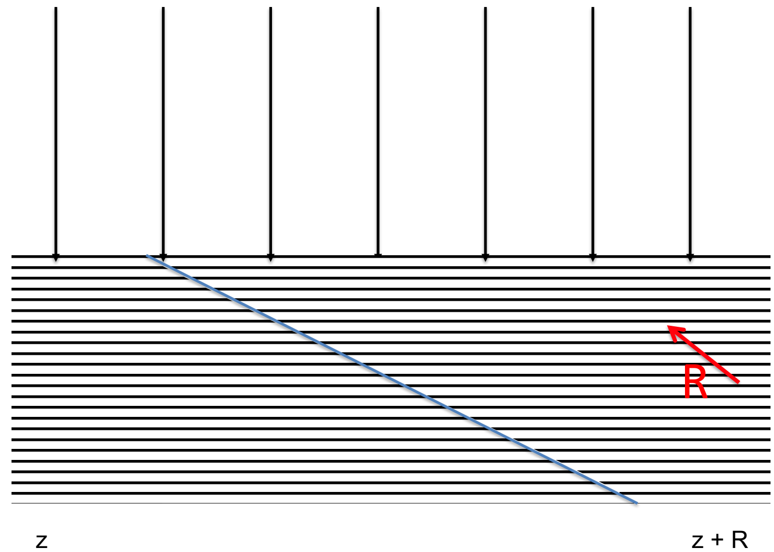

37

Zaluzec - 2023

Simple Linear Defect Stacking Fault

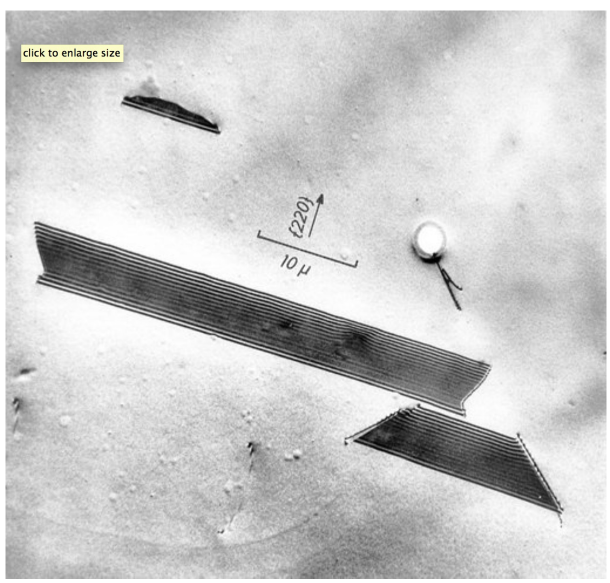

A
B
C
A
B
C
B
C
A
B
C
A
A
B
C
A
B
C

38

Defect Studies / Imaging Displacement Fields

Howie Whelan Equations

$$\frac{d\phi_0}{dz} = \left[\frac{\pi i}{\xi_0}\right]\phi_0 + \left[\left(\frac{\pi i}{\xi_g}\right)e^{2\pi i(sz+\vec{g}.\vec{R}(z))}\right]\phi_g$$

$$\frac{d\phi_g}{dz} = \left[\frac{\pi i}{\xi_0}\right]\phi_g + \left[\left(\frac{\pi i}{\xi_g}\right)e^{-2\pi i(sz+\vec{g}.\vec{R}(z))}\right]\phi_0$$

s•z ⇒ s•z + g•R(z)

g• R controls diffraction contrast for crystalline defects
R(z)= 3D displacement field of the defect

Planar Defects

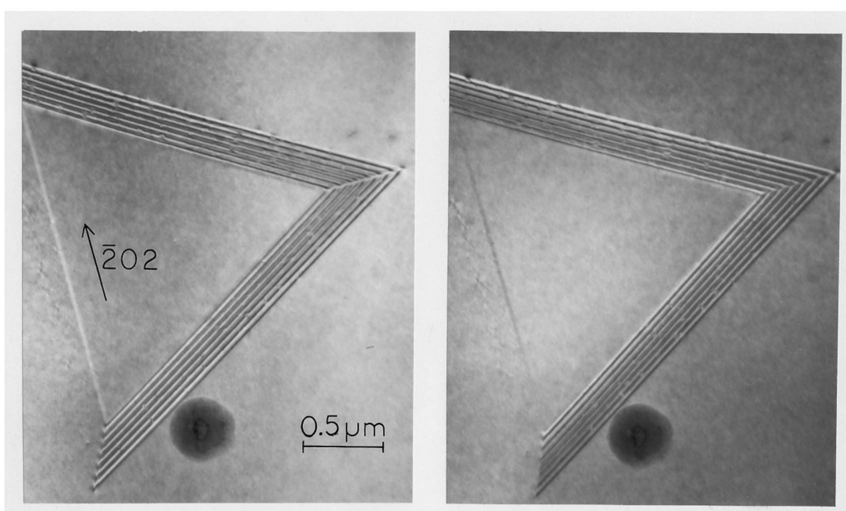

g.R = 0, 1, 2 … No Contrast
g.R < $\pm$ $2\pi/3$ Oscillitory Contrast
Symmetric BF, Asymmetric DF

Symmetry of the stacking faults images

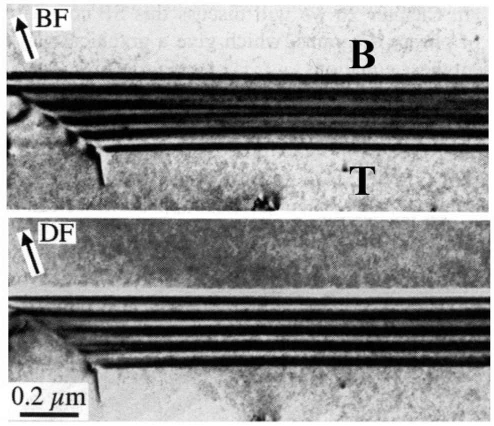

-The fringes at the top are the same in BF and DF images
-The fringes at the bottom are complementary

Dislocation Images

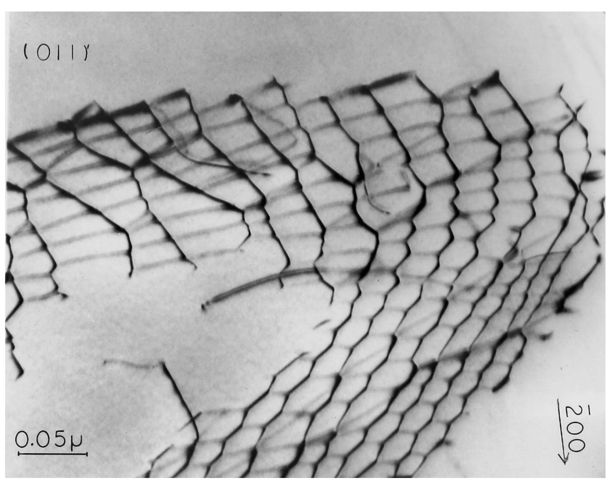

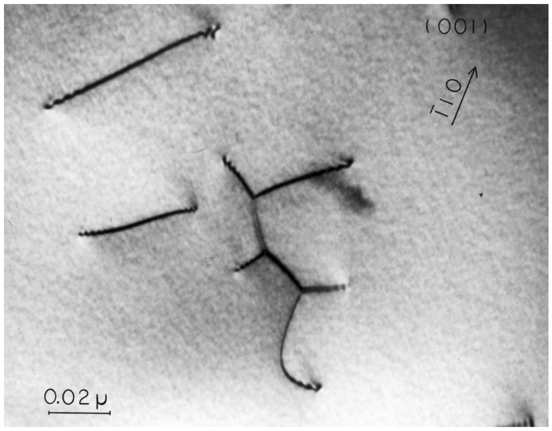

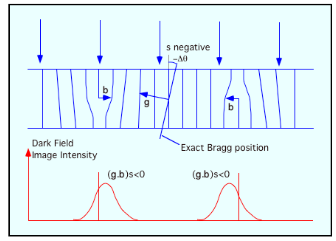

$$\phi_g = \left(\frac{\pi i}{\xi_g}\right)\int_0^t e^{-2\pi i (s_g z + \vec{g}\bullet\vec{R})}dz$$

$$\xi_g = \pi V_c \frac{\cos(\theta)}{\lambda F(\theta)}$$

R = displacement of the unit cell in the area of the defect due to its strain field
g = diffracting vector used in imaging.

Contrast of Dislocations due to local changes in orientation of planes - recall Bend Contours

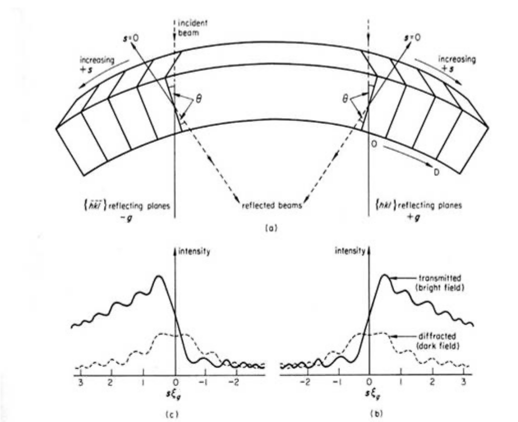

(a) A thin crystal bent into a large radius showing reflection from the opposite sides of the same set of (*hkl*) crystal planes. (b), (c) The intensity distribution versus position for BF and DF (rocking curves). (d) The BF image corresponding to (a). (e), (f) are SADPs showing opposite two-beam diffracting conditions at Y and X in (d)

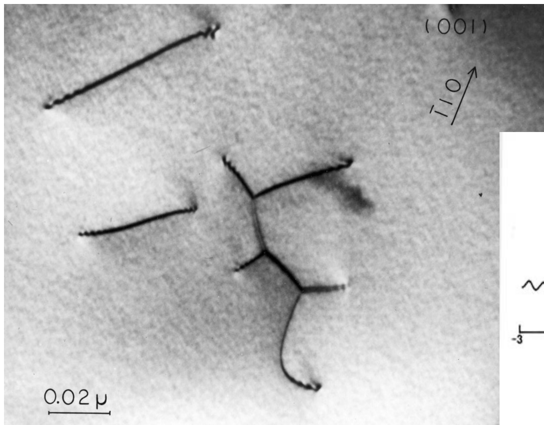

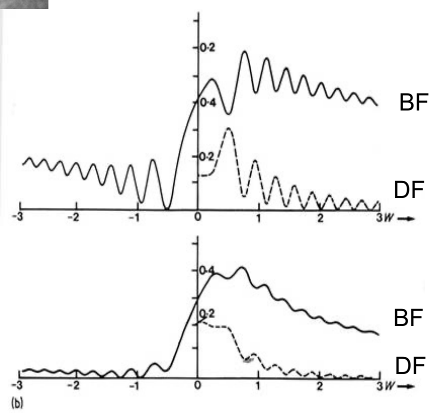

FIG. 3.5

Rocking curves calculated for (i) $\xi_g/\xi_g' = 0.05$ and (ii) $\xi_g/\xi_g' = 0.1$ showing the bright-field curves (full line) are asymmetric about w = 0, whereas the dark-field (broken lines) are symmetrical.

Maximize Contrast with W > 0.
Dark Field Images are Symmetric

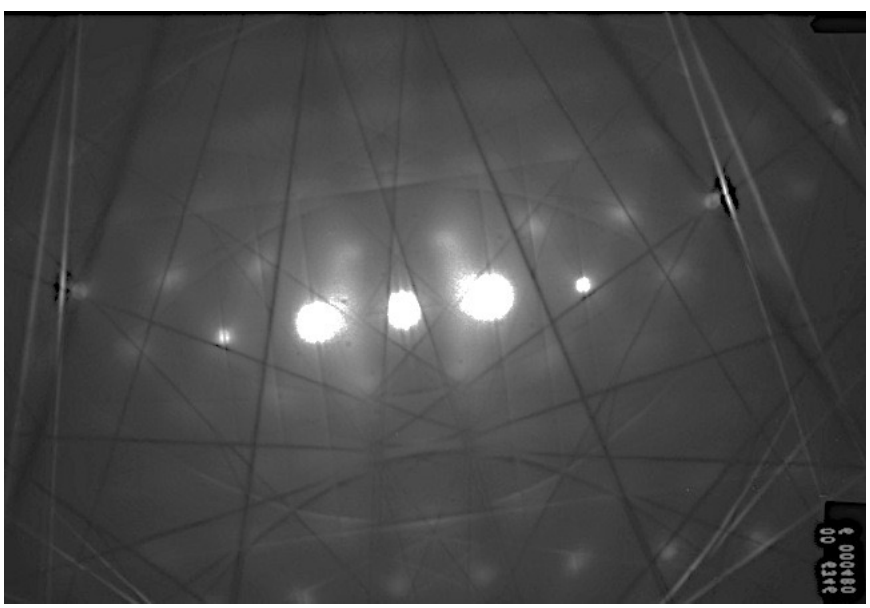

s > 0

s = 0

s < 0

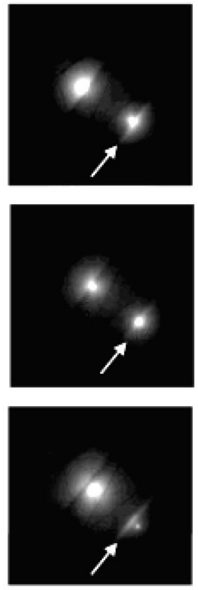

Orientation Dependent
Scattering (Contrast) Studies

$$\phi_g = \left(\frac{\pi i}{\xi_g}\right)\int_0^t e^{-2\pi i(s_g z + \vec{g}\bullet\vec{R})}dz$$

$$\xi_g = \pi V_c \frac{\cos(\theta)}{\lambda F(\theta)}$$

R = displacement vector
g = scattering direction

g•R
controls diffraction contrast
for crystalline defects

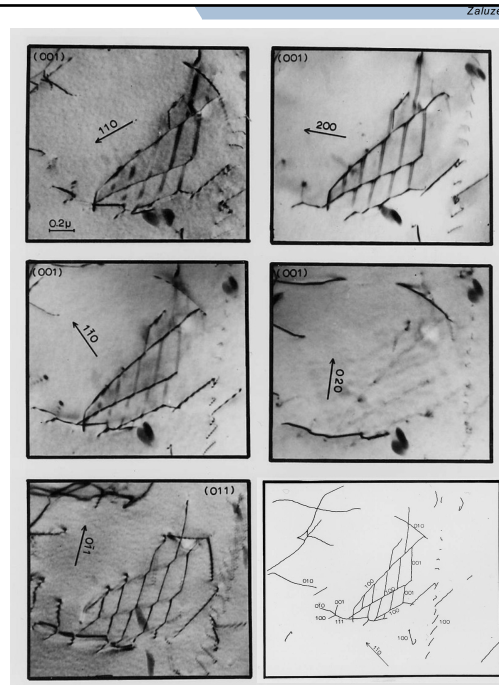

(1) Dislocations are most easily visible and the images broadest when $\mathbf{s} = 0$. Images for which $\mathbf{g \cdot b} \geqslant 2$ show much stronger contrast for the same value of $\mathbf{s}$ than those for which $\mathbf{g \cdot b} = 1$ or 0. At $\mathbf{s} = 0$, images for which $\mathbf{g \cdot b} = 2$ show double images, and as $\mathbf{s}$ is increased one of the images fades away. Images for which $\mathbf{g \cdot b} = 0$ also show double images at $\mathbf{s} = 0$ but the two peaks fade away together as $\mathbf{s}$ is increased. The images for which $\mathbf{g \cdot b} = 1$ also fade away as $\mathbf{s}$ is increased and become so much weaker than images for which $\mathbf{g \cdot b} = 2$ that they can be confused with images for which $\mathbf{g \cdot b} = 0$. Because the background intensity in dark field becomes very small at large values of $\mathbf{s}$ (cf. Fig. 5.3(b)) weak images can be observed as bright lines on a dark background. At small values of $\mathbf{s}$ the bright and dark field images appear qualitatively similar.

(2) Dislocations running from top to bottom of a foil show oscillatory contrast when imaged at $\mathbf{s} \sim 0$. This contrast is damped out as $\mathbf{s}$ is increased. Images taken in bright field with a given diffracting vector give similar oscillatory contrast to that observed in dark field for the same sense of $\mathbf{g}$ for the part of the dislocation at the top of the foil.

(3) The image of a dislocation lies to one side of a dislocation provided $\mathbf{g \cdot b} \neq 0$ and $\mathbf{s} \neq 0$. The origin of this can be seen from simple diagrams representing the strain fields around dislocations. The displacements on one side of an edge dislocation can be seen to rotate the crystal towards the Bragg condition (thus giving strong contrast) and on the other side away from this condition. The side to which the image lies is given by the sign of $(\mathbf{g \cdot b})\,\mathbf{s}$ and the magnitude of the shift by the magnitude of $(\mathbf{g \cdot b})\,\mathbf{s}$. Thus when $\mathbf{g \cdot b} = 0$ the image is centred on the dislocation. An indication that $\mathbf{g \cdot b} = 0$, even when this condition gives strong residual contrast can therefore be obtained by reversing $\mathbf{g}$; the absence of an image shift for $|s\xi| > 1$ implies that $\mathbf{g \cdot b} = 0$.

(4) The image of a dislocation reverses top to bottom and side to side if $\mathbf{g}$ is reversed. A closely spaced dislocation dipole can give apparently more complex behaviour on reversing $\mathbf{g}$ since the images of the dislocations may overlap.

Loretto

49

49

g[hkl]	b[hkl]	g.b
[100]	[100], [010], [001]	1 , 0 , 0
[110]	[100], [010], [001]	1, 1, 0
[111]	[100], [010], [001]	1, 1, 1
[110]	[110], [101], [011]	2, 1, 1
[1-10]	[110], [101], [011]	0, 1, -1

0 = Out of Contrast 1 = In-Contrast 2 = Double Contrast

50

50

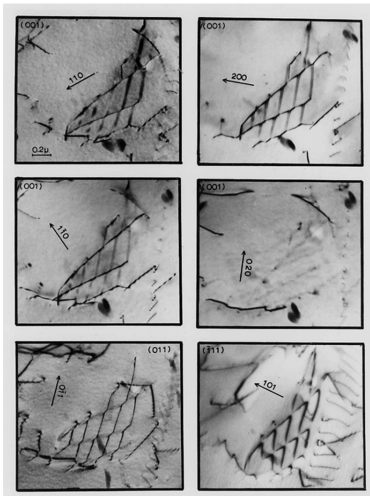

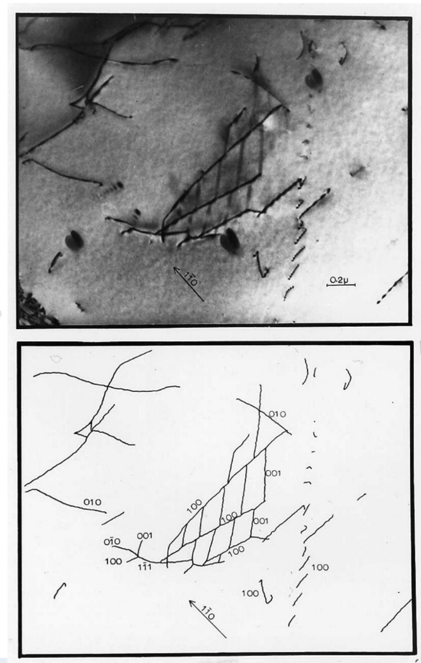

51

Single-title holder
Double-tilt holder
Low-background holder
Heating holder
Cooling holder
Cryo-transfer holder

Specimen Holders

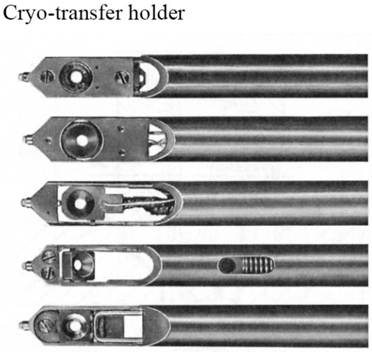

Figure 8.8. Examples of different designs for the side-entry holder. From the top, they are: a rotation holder, a heating holder, a cooling holder, a double-tilt holder, and a single-tilt holder.

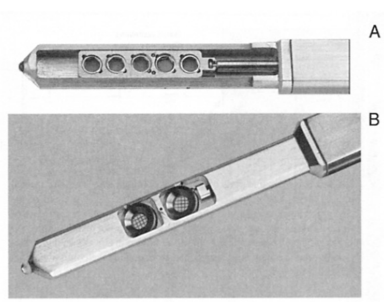

Figure 8.9. Multiple-specimen holders. (A) Five-specimen single-tilt and (B) two-specimen double-tilt.

52

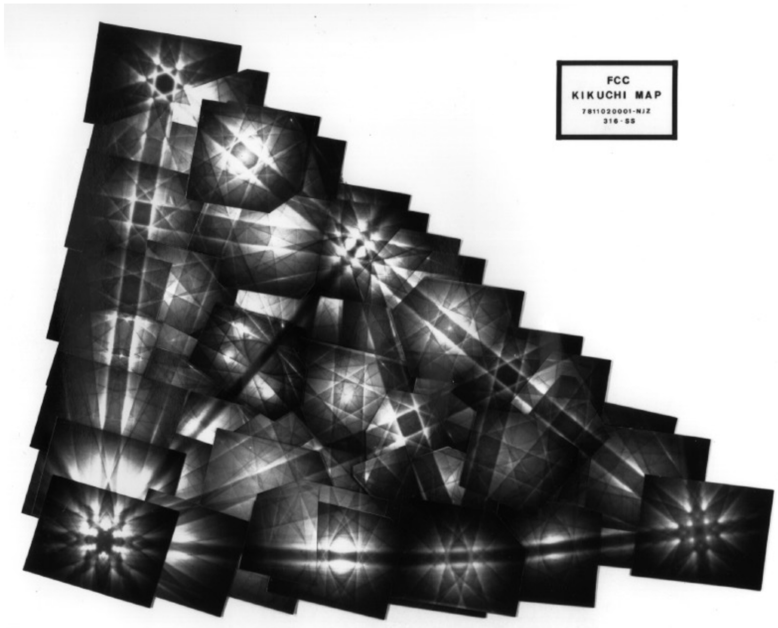

Dislocation Images: Expt vs Calculation

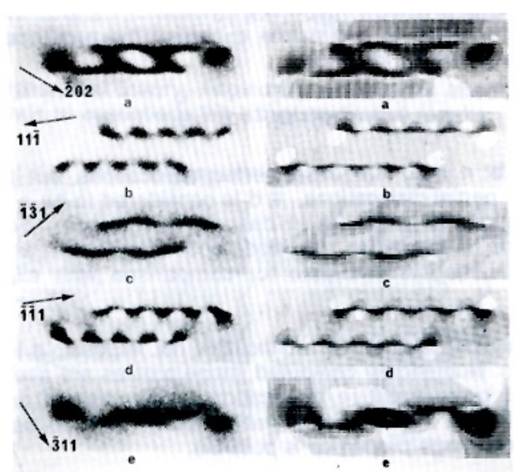

Figure 1.49 Examples of the quantitative agreement that can be achieved between observed and computed dislocation images. Left: observed images for different diffraction vectors Right: corresponding computer generated images.

Dislocation Images: Expt vs Calculation

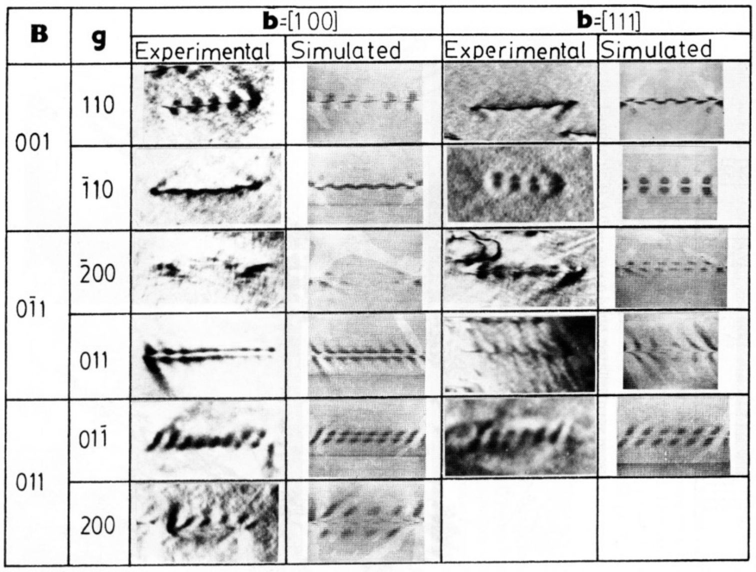

Dislocation Loops

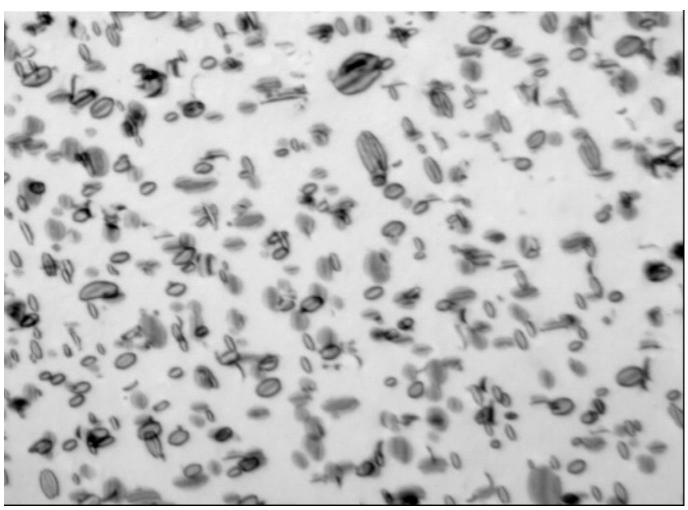

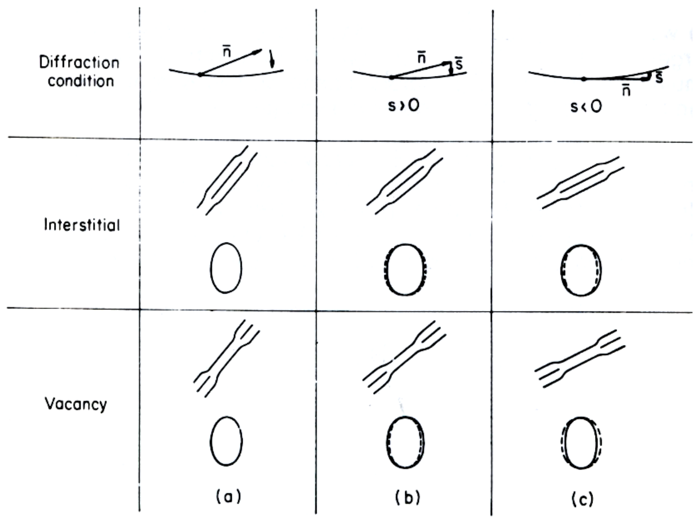

Figure 1.68 Contrast experiment allowing to determine the nature of dislocation loops. Diffraction vector n. The foil is tilted in the indicated sense.

Careful Experiments are needed in Loop Analysis

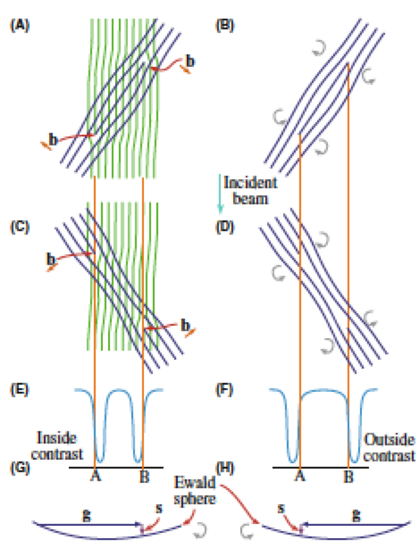

Williams & Carter

HREM
Phase Contrast Imaging

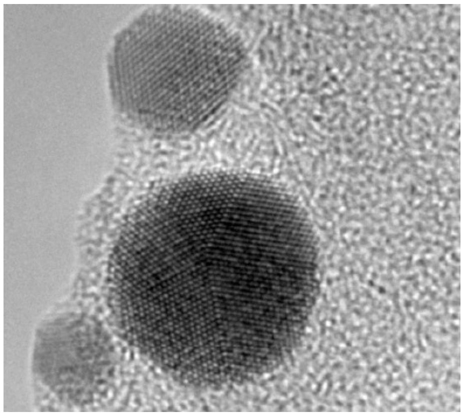

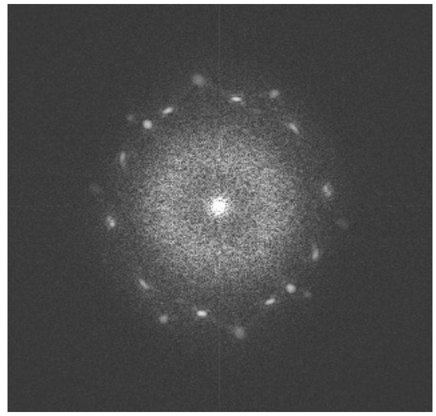

Amplitude/Diffraction Contrast	Phase Contrast

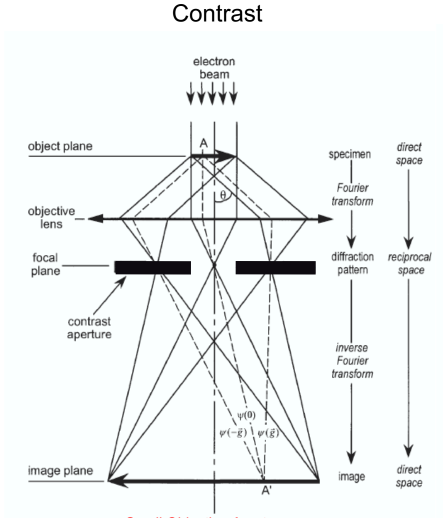

Small Objective Aperture
Intensities of either Unscattered Electrons or individual Scattering Events are used to form an Image
Intensity from other Beams is lost

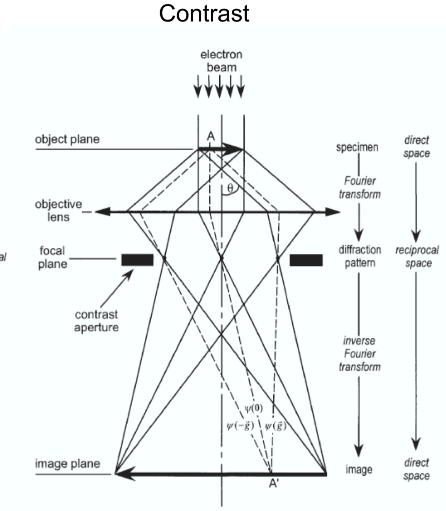

Large or No Objective Aperture
Phases/Intensities of Scattered Electrons are combined to form an Image

Zaluzec - 2023

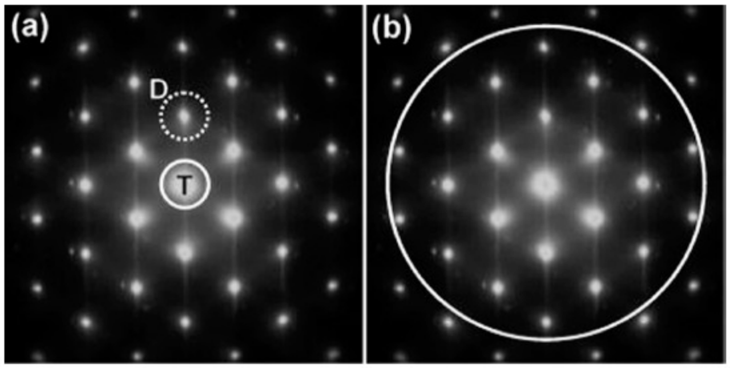

Fig. 6. The size and the position of the objective aperture for diffraction contrast (a) and phase interference contrast (b)

61

61

Zaluzec - 2023

Image Formation in the High-Resolution TEM

- In the high-resolution TEM, the incident electron beam interacts strongly with the crystal, forming multiple diffracted beams that are brought together by the objective lens so they can interfere to create an image.
- ***TEM images are able to depict the projected atom columns because they are interference patterns of the directly transmitted beam with beams diffracted from the specimen.***
- Structural information from the specimen is encoded in the phase of the scattered electron waves [5]. Although the electron phase is not an observable (it is not gauge invariant [6]), phase differences can be measured by interference experiments such as imaging.
- At the "optimum" or "extended Scherzer" defocus [7], objective lens phase shifts allow interference of the scattered electron waves exiting the specimen to turn the relative phases of the waves into image peaks mapping the atom positions (at the resolution of the microscope).

[5] J.M. Cowley, Diffraction Physics (1975) North Holland / American Elsevier.
[6] H. Rose, Lectures on Charged Particle Optics, LBNL (2004)
[7] O. Scherzer, J. Appl. Phys. 20 (1949) 20-29.

62

62

Simplest HREM Imaging
2 Beam Lattice

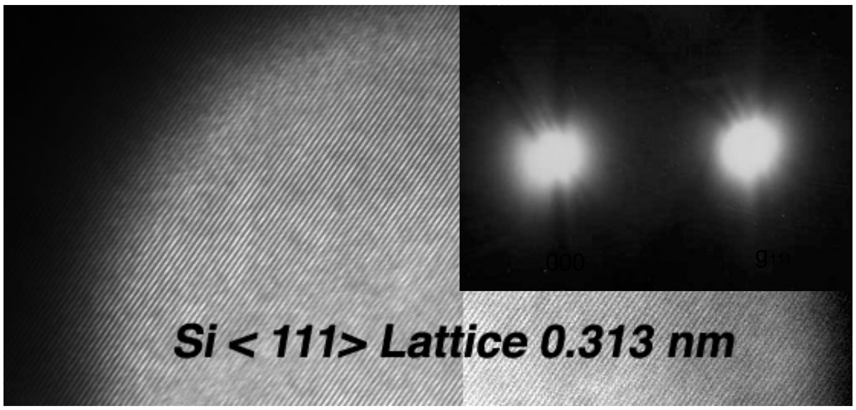

63

off-axis lattice fringe imaging

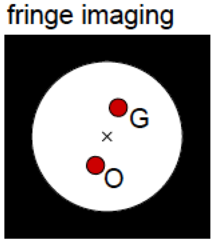

s = 0 and g’ = g

on-axis 3-beam imaging

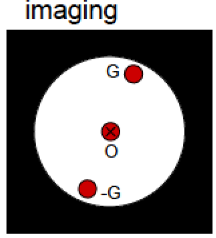

s ≠ 0

on-axis many-beam imaging

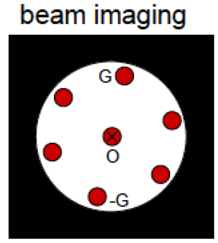

s ≠ 0

64

Zone Axis Images
All the “diffracted beams” interfere

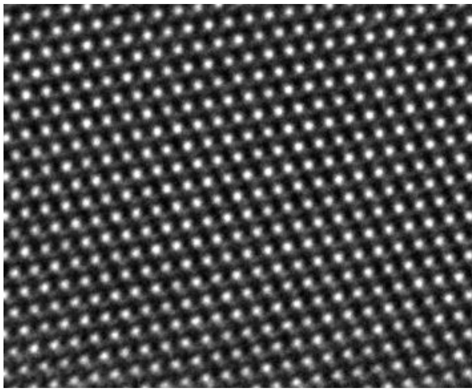

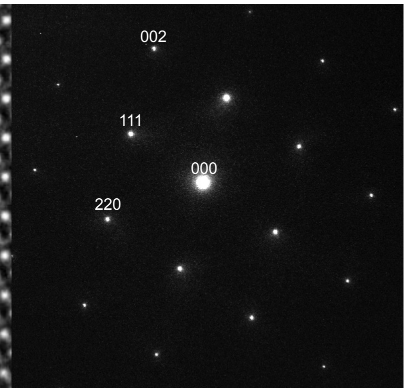

Silicon {110}
$d_{<111>}$ = 0.3134
$d_{<220>}$ = 0.1919
$d_{<002>}$ = 0.1635

Gold – HREM Images

Small Variations
in Orientation and Thickness

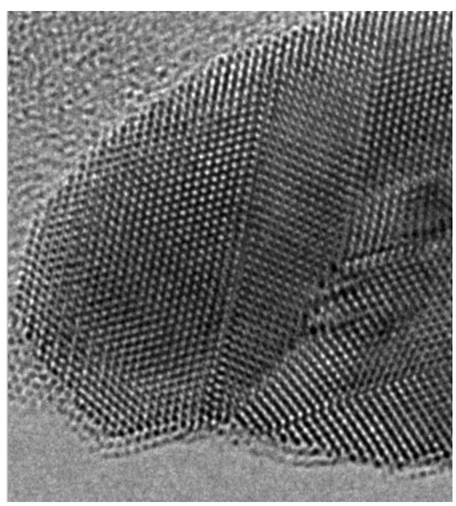

Significant Variations
in Orientation and Thickness

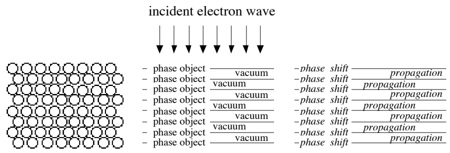

$$\psi(x,y)_V = \psi_{in}(x,y)_0 \exp\left(\sigma\int_0^{\varepsilon} V(xy,z)dz\right) = \psi_{in}(x,y)_0 \exp\left(i\sigma V_p(xy)_1\right)$$

$$\psi(x,y)_n \approx \frac{\exp ik'\varepsilon}{\varepsilon}\left[\psi_{in}(X,Y)_{n-1} \exp\left(i\sigma V_p(X,Y)_n\right)\right] \otimes \exp\left[\frac{ik'\varepsilon}{2\varepsilon}(X^2+Y^2)\right]$$

Phase of the exit wave depends upon the thickness & interference of the diffracted and transmitted beams in the specimen.

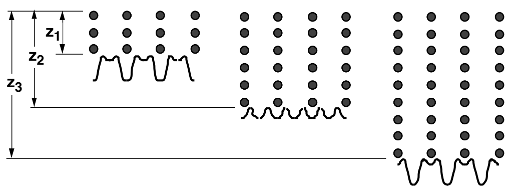

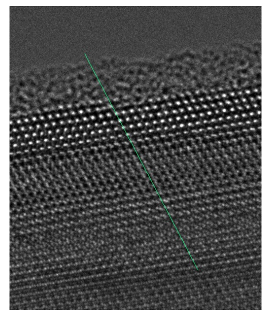

Dark Atoms

White Atoms

Silicon {110} – Variable Thickness
Amorphous Material at Edge

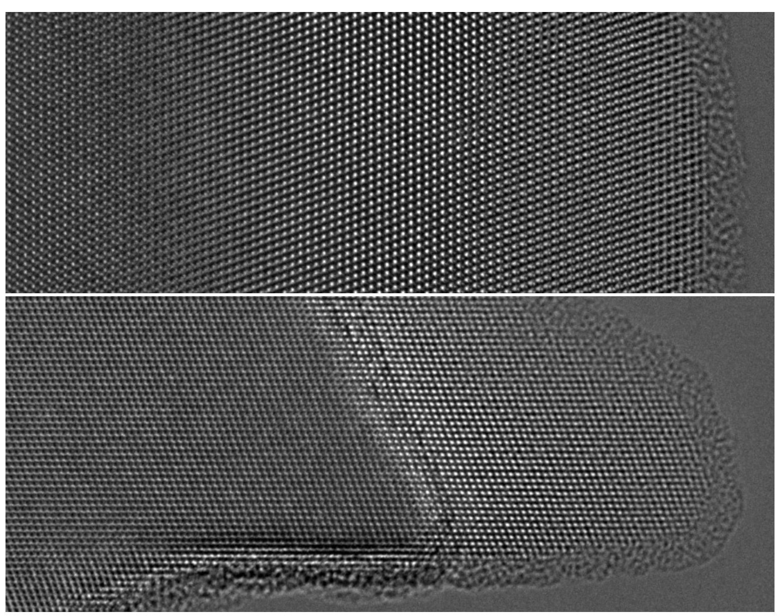

STO/LMO

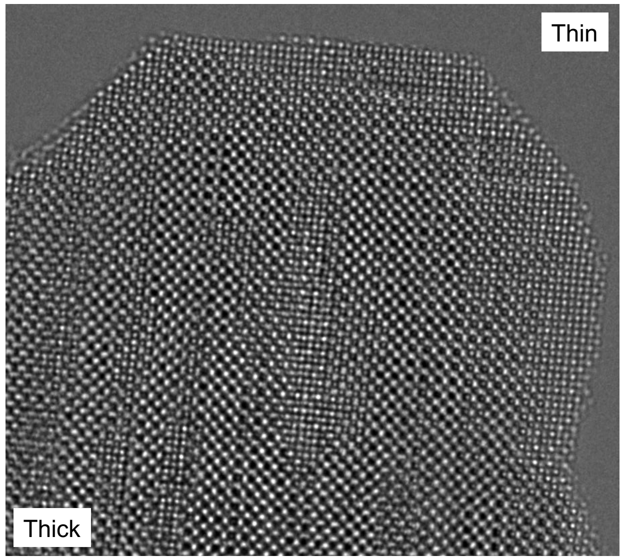

Excellent Clean Surface!

STO/LMO

Not So Clean!
(but in reality not “bad”)

Si

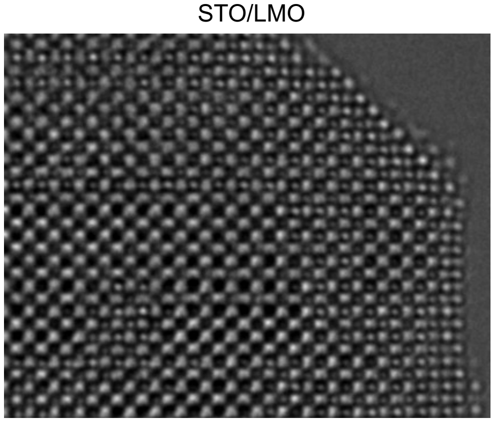

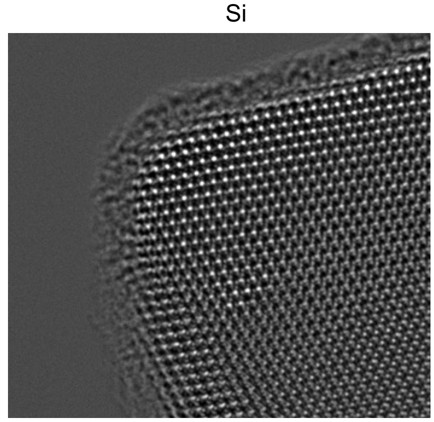

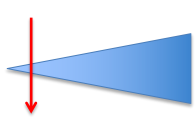

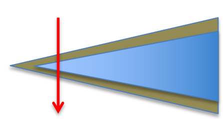

Phase Contrast Change
with thickness and with defocus

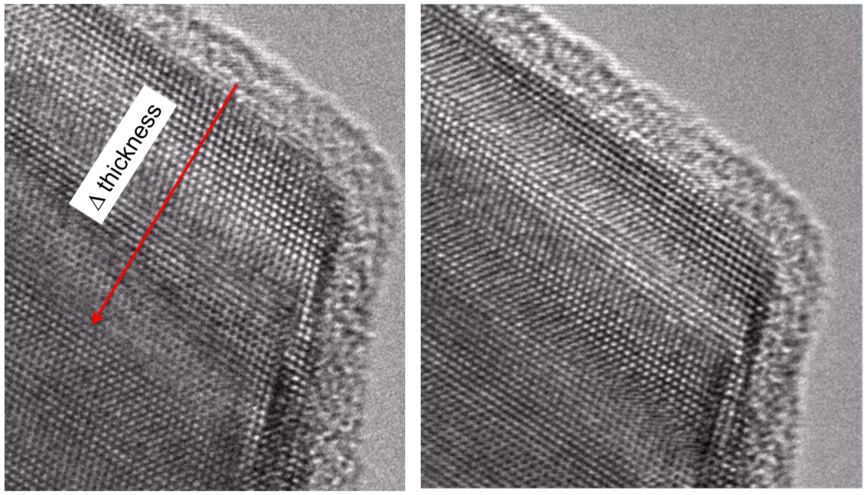

Δ focus

To interpret HREM you MUST calculate the EXIT wave function
then compare with experimental images

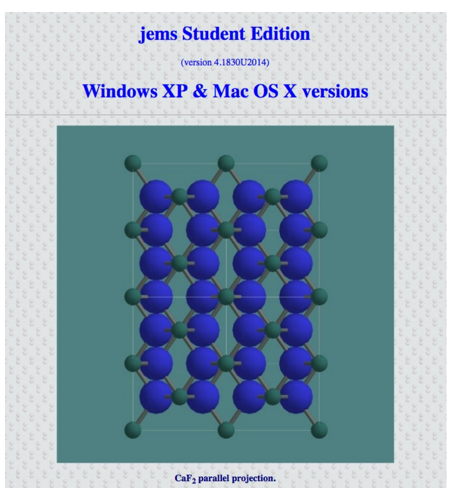

http://www.jems-saas.ch

Pierre Stadelmann
pierre.stadelmann@epfl.ch

E-mail: jems.saas@gmail.com
info@jems-saas.ch

Address: JEMS-SAAS
Dr. P. Stadelmann
Obere Lomattenstrasse 33
CH-3906 **Saas-Fee**
Switzerland

Multislice Method

1. divide the sample up into thin slices
2. project the potential of a slice onto a plane within that slice: this a phase grating
3. calculate the amplitudes and phases of all the beams resulting from the incident beam interacting with the projected potential
4. propagate these beams through the microscope until they reach the next slice
5. Calculate a new set of beams

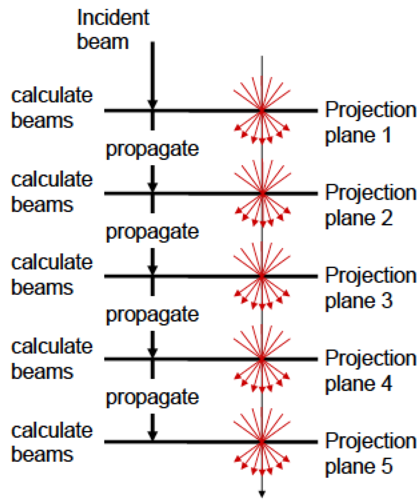

73

73

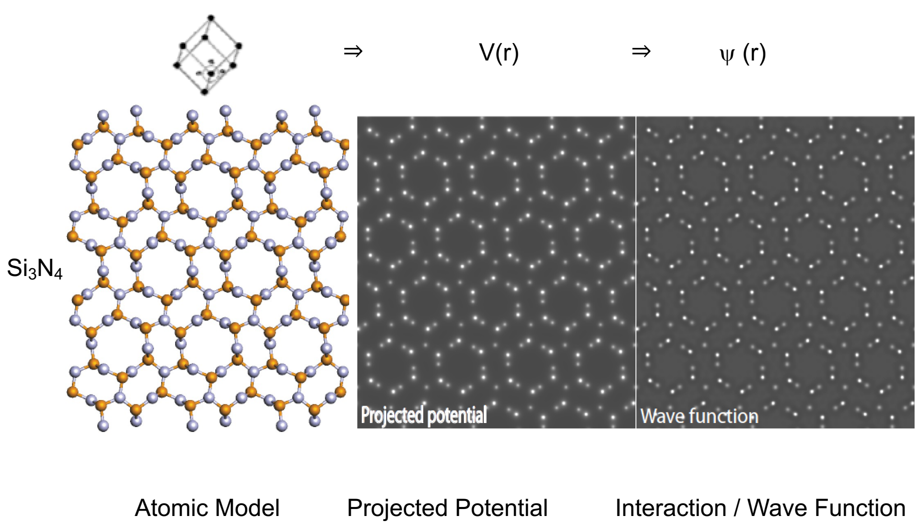

74

74

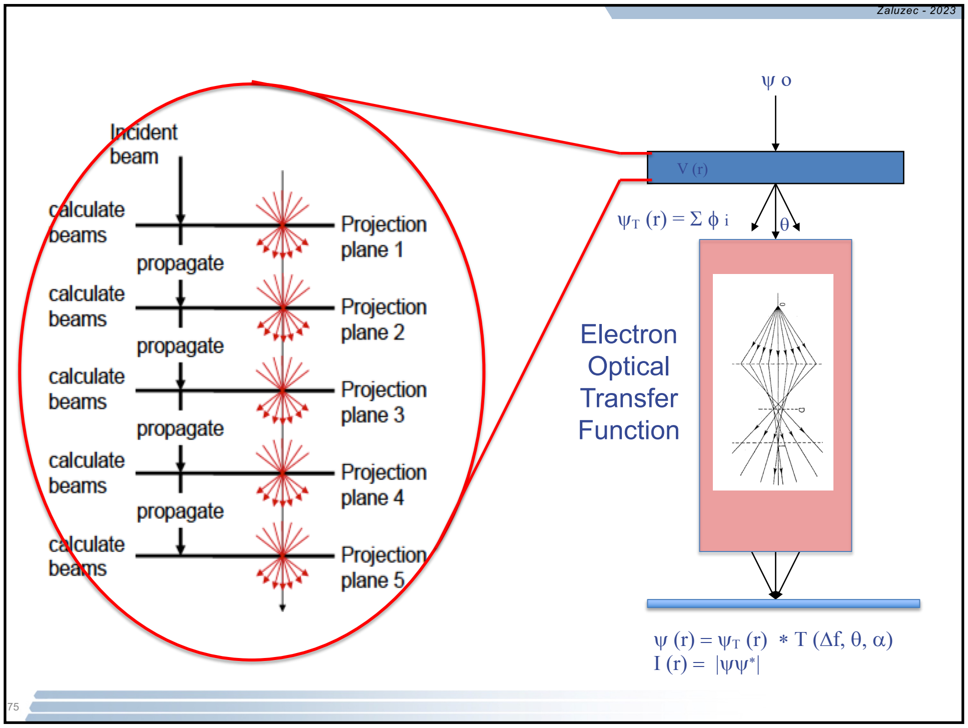

75

Imaging Lenses Introduce Phase Shifts due to:

Defocus (Δf)	$\chi_2(\theta,\Delta f) = -\frac{2\pi}{\lambda}\Delta f\frac{\theta^2}{2}$ $\Delta f = -1{,}2\sqrt{C_s\lambda}$ Scherzer Defocus
Spherical Aberration (C_s)	$\chi_1(\theta) = -\frac{2\pi}{\lambda}C_s\frac{\theta^4}{4}$
Contrast Transfer Function	$T_C(\theta,\Delta f) = \exp i(\chi_1+\chi_2) = \exp i\left\{-\frac{2\pi}{\lambda}\left(C_s\frac{\theta^4}{4}+\Delta f\frac{\theta^2}{2}\right)\right\}$
Chromatic Aberration (C_c) (Temporal Coherence)	$E_T = \exp\left\{-\frac{\pi^2}{\lambda^2}(\Delta u)^2\theta^4\right\}$ $\Delta u = C_c\left[\left(\frac{\Delta V}{V}\right)^2+\left(\frac{2\Delta I}{I}\right)^2+\left(\frac{\Delta E}{E}\right)^2\right]^{1/2}$
Spatial Coherence (Beam Convergence)	$E_S = \frac{2J_1(x)}{x}$ $x = 2\pi\alpha\left\{\Delta f\frac{\theta}{\lambda}+\left[\lambda C_s - i\pi(\Delta u)^2\right]\frac{\theta^3}{\lambda^2}\right\}$
Total / System Transfer Function	$T_R = T_C \,.\, E_T \,.\, E_S$
Wave Function at the Detector Plane	$\tilde{\psi}_E(\vec{q})T(\vec{q},\Delta f)$

76

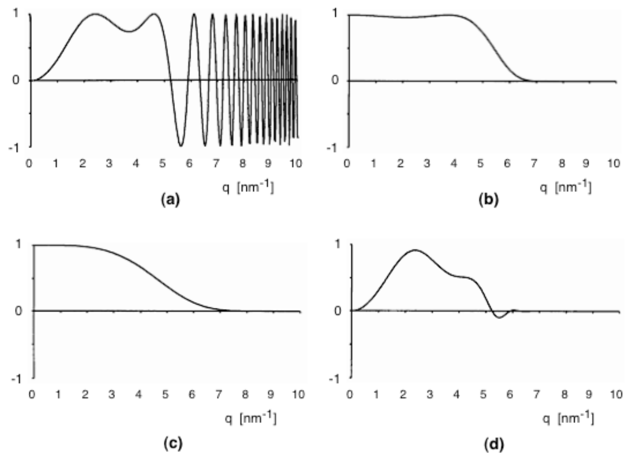

Fig. 8 : *Transfer function and its envelopes (Scherzer defocus)*

a) contrast transfer function
b) spatial coherence envelope
c) temporal coherence envelope
d) product (a)(b)*(c) – tranfer function in amplitude*

Calculated Images (JEMS – P. Stadelmann)

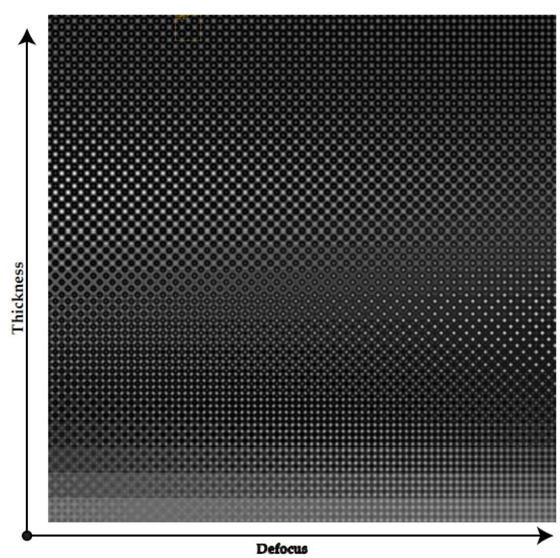

Phase Transfer in the High-Resolution TEM

Phase Contrast Transfer Function shows strength of transfer into image

$$\Delta f \approx -1.2\sqrt{C_s \lambda}$$

$$\delta \approx 0.67 C_s^{1/4} \lambda^{3/4}$$

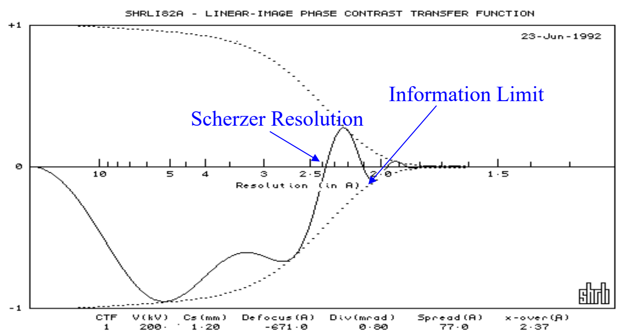

Same-sign transfer defines microscope resolution

in the "thin WPOA" Negative PCTF = Dark Atoms on Light Bgnd

in the "thin WPOA" Positive PCTF = Bright Atoms on Dark Bgnd

End of transfer is the microscope's "information limit"

Temporal & Coherence Envelope Effects

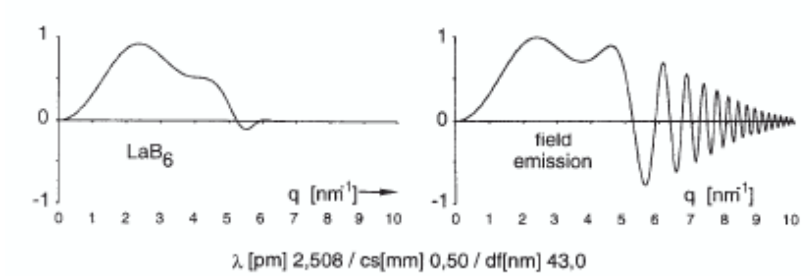

Temporal Coherence = 2 E λ / ΔE
Spatial Coherence = λ / 2α

70 um SS 3 | 30 um SS 3

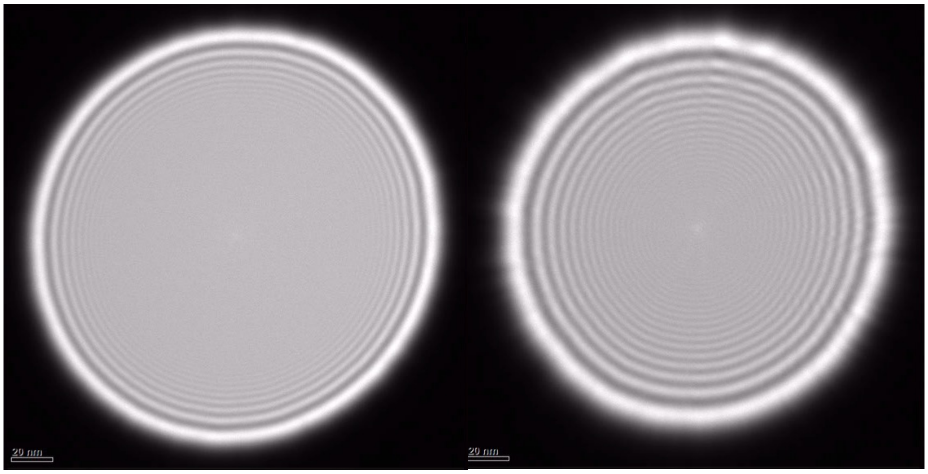

Coherence of the Source Improves your Images at High Resolution

81

81

Information Delocalization
Different Diffracting Beams are Brought to Focus
At Different Locations due to Aberrations of the Objective Lens

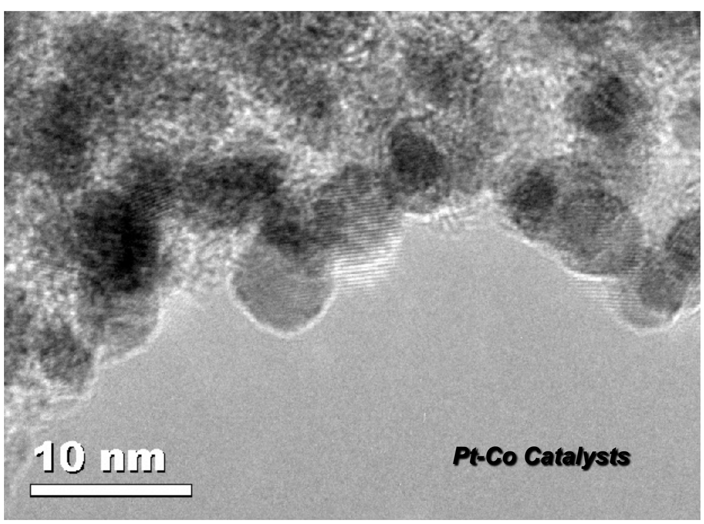

$$\textit{Delocalization} : R = | C_5 \lambda^5 g^5 + C_3 \lambda^3 g^3 + \lambda \Delta f\, g |_{max}$$

82

82

What are the limitations in Elastic/Inelastic Imaging & Spectroscopy ?

Aberrations

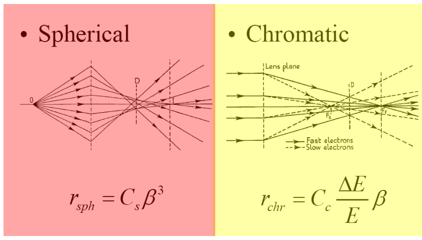

$$r_{sph} = C_s \beta^3$$

$$r_{chr} = C_c \frac{\Delta E}{E} \beta$$

The source and solution to "resolution limitations" has been known for nearly 50 years

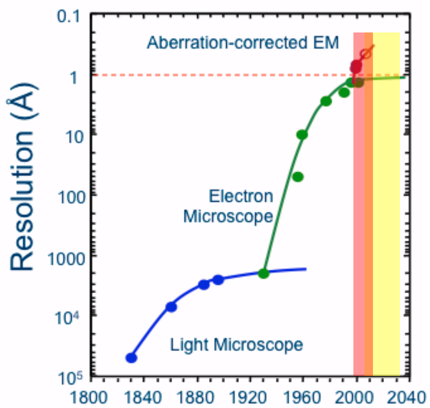

EM Imaging
w / wo Image Corrector

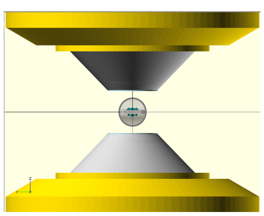

PCTF ACTF

C_1 -84 nm
C_3 2.7 mm
C_5 -2mm
C_c 2.7 mm
E_o 300 kV

C_1 -8 nm
C_3 25 um
C_5 -2mm
C_c 300 um
E_o 300 kV

C_1 -1 nm
C_3 10 um
C_5 2mm
C_c 300 um
E_o 200 kV

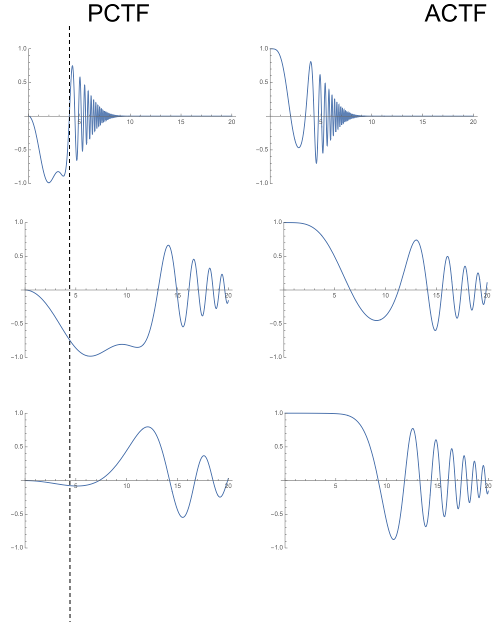

Using δf, C_s, C_c now have a new tool for Manipulating Contrast

First Generation Corrected Instruments
C_s Only

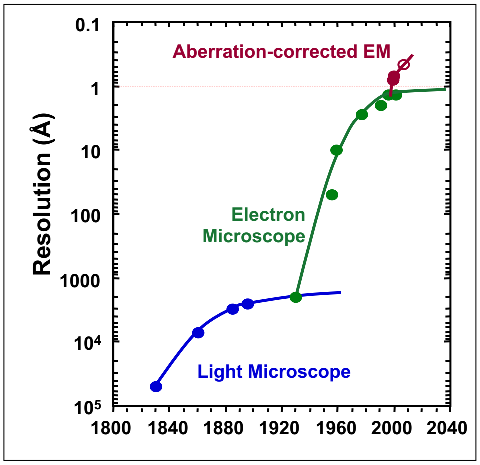

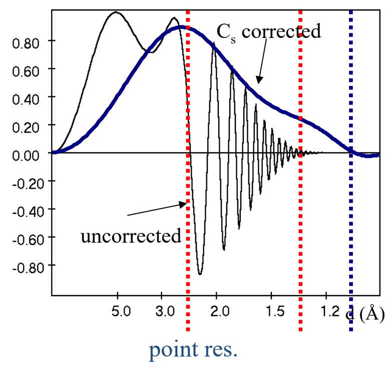

Hyperspectral Imaging & Spectroscopy
A view from the Trenches
Where are the game changers?

- C_s Correction is now routine !
- C_c Correction is it important ?
  - exists only at limited number of Institutions
  - wrt to resolution has largest impact on lower voltages
  - What else does aberration correction impact – Contrast!

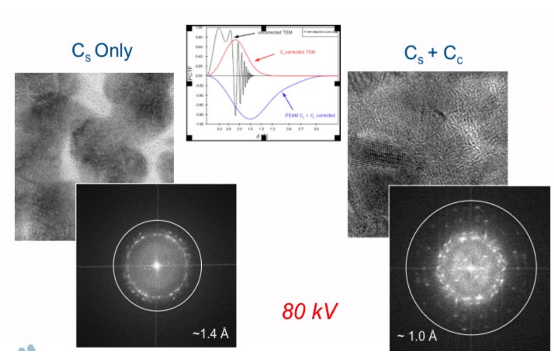

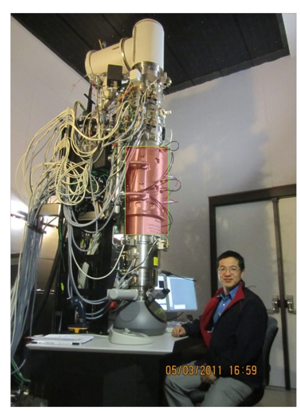

Argonne Chromatic Aberration-corrected TEM (ACAT)

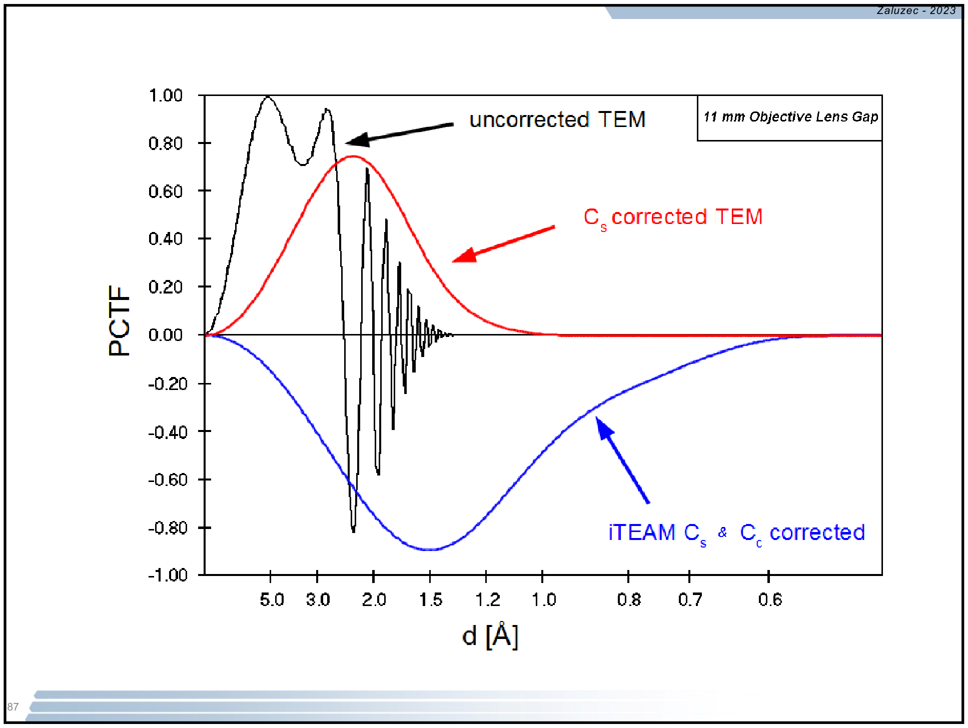
Zaluzec - 2023
11 mm Objective Lens Gap
uncorrected TEM
C_s corrected TEM
iTEAM C_s & C_c corrected
PCTF
1.00
0.80
0.60
0.40
0.20
0.00
-0.20
-0.40
-0.60
-0.80
-1.00
5.0
3.0
2.0
1.5
1.2
1.0
0.8
0.7
0.6
d [Å]
87

87

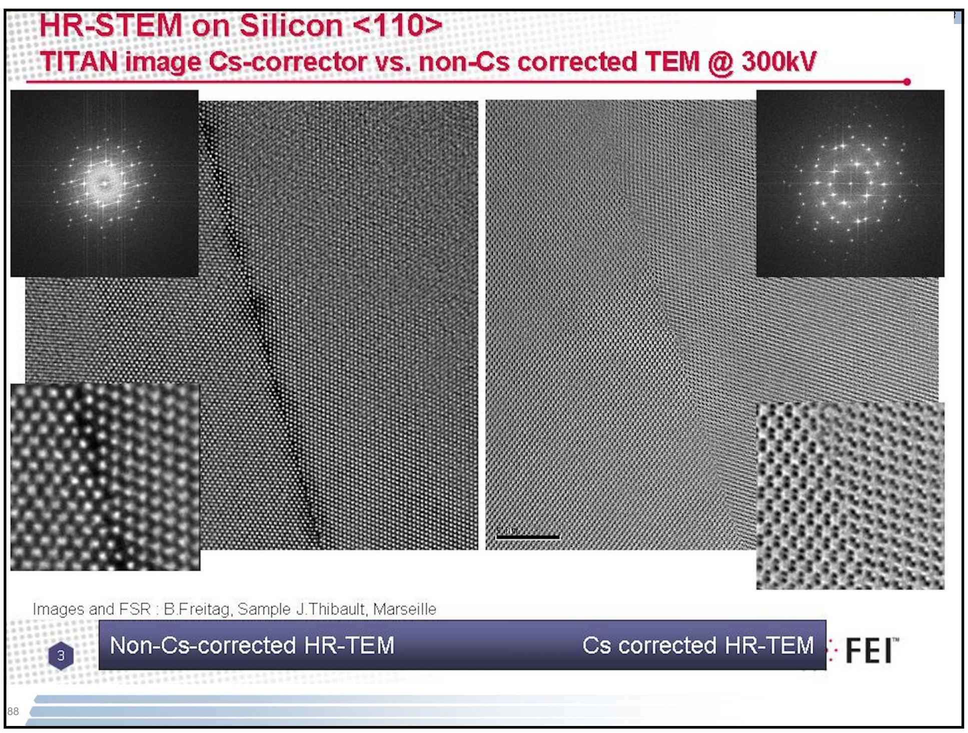
HR-STEM on Silicon <110>
TITAN image Cs-corrector vs. non-Cs corrected TEM @ 300kV
Images and FSR : B.Freitag, Sample J.Thibault, Marseille
Non-Cs-corrected HR-TEM
Cs corrected HR-TEM
FEI
3
88

88

Amplitude vs Phase Contrast Imaging

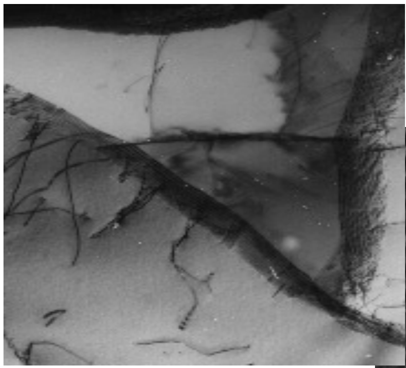

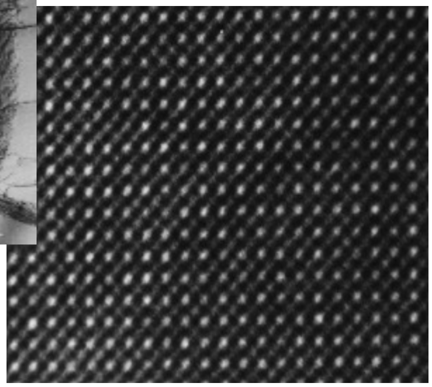

C_S Correction is Phase Correction HREM "Phase Contrast" is the most common mode

- To get information beyond Scherzer resolution requires a "correction" of the phase changes introduced by spherical aberration.
- Correction may be by hardware, or by software such as focal-series reconstruction of the exit-surface wave.
- Early focal-series reconstruction methods used simple linear combinations of image intensities at different spatial frequencies to correct for spherical aberration and extend microscope resolution.

Contrast & Information Transfer: TEM

Contrast Transfer function

$$T_{phase}(q) = \sin\left(\frac{(2\pi)}{\lambda}\left(\frac{1}{2}C_1\lambda^2q^2 + \frac{1}{4}C_3\lambda^4q^4 + \frac{1}{6}C_5\lambda^6q^6 + \frac{1}{8}C_7\lambda^8q^8\right)\right) * E_t * E_s;$$

$$T_{amplitude}(q) = \cos\left(\frac{(2\pi)}{\lambda}\left(\frac{1}{2}C_1\lambda^2q^2 + \frac{1}{4}C_3\lambda^4q^4 + \frac{1}{6}C_5\lambda^6q^6 + \frac{1}{8}C_7\lambda^8q^8\right)\right) * E_t * E_s;$$

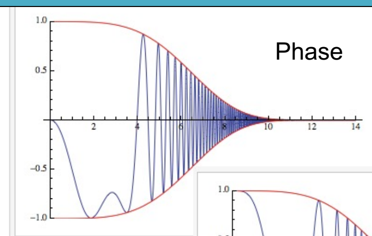

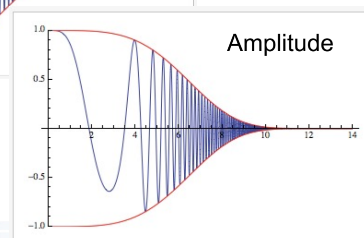

E_t: damping envelope of temporal coherence

E_s: damping envelope of spatial coherence

C_1: defocus - Δf

C_3: Spherical Aberration Coefficient

C_5, C_7: Higher Order Aberration Coefficients

Information limit:

temporal coherence $\rightarrow$ C_c, ΔE

91

91

Zaluzec - 2023

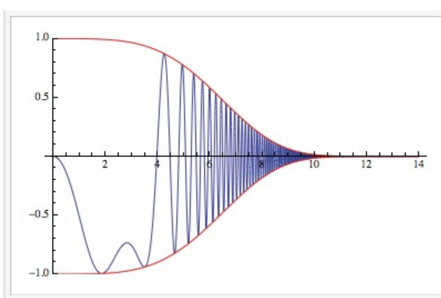

Aberration Correction &
Conventional HREM
– Phase Contrast

$C_1 = \delta f$

C_3 1.5 -> 0.1 mm

C_c ~ 1.5 mm

C_5 ~ - 2 mm

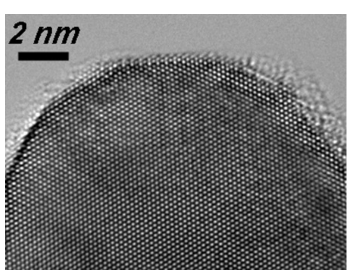

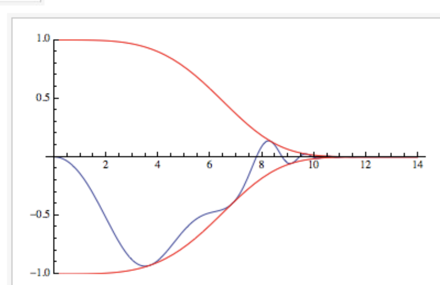

92

92

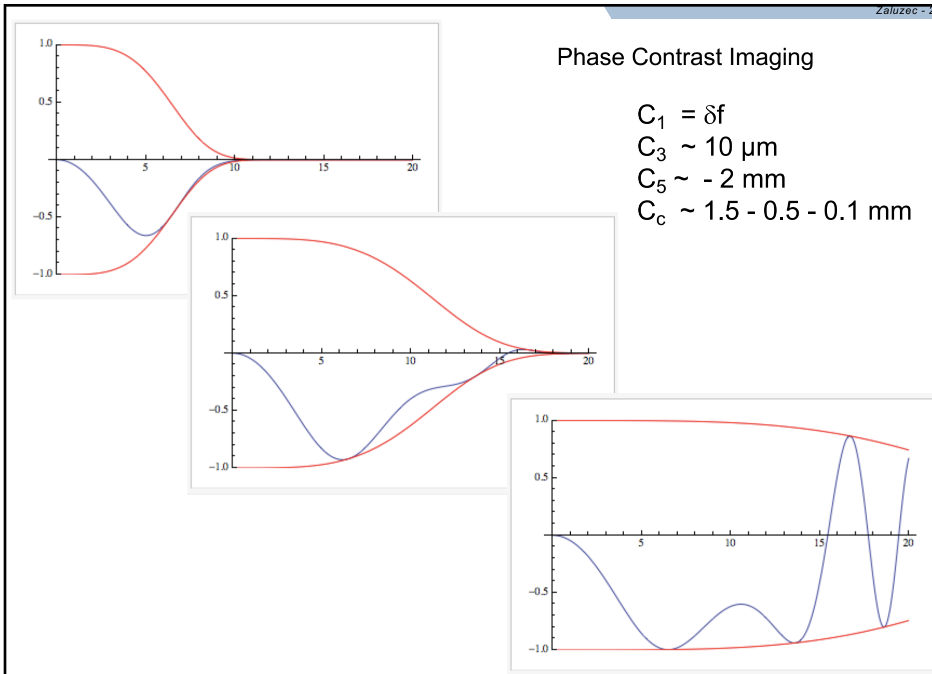

Phase Contrast Imaging

$C_1 = \delta f$
$C_3 \sim 10\ \mu m$
$C_5 \sim -2\ mm$
$C_c \sim 1.5 - 0.5 - 0.1\ mm$

93

93

Aberration Free Imaging

Influence of Contrast Delocalization

Uncorrected : $C_s = 1.2$ mm

Corrected : $C_s = 0.05$ mm

$\Delta f = -257$ nm; $R = 1.4$ nm

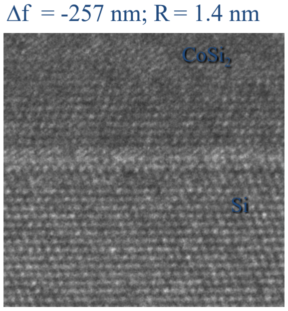

focus of least confusion

$\Delta f = -68$ nm; $R = 4.4$ nm

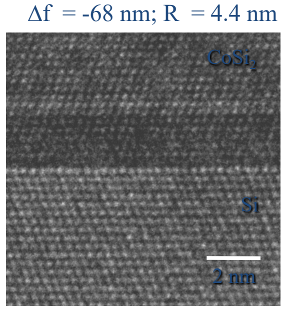

Scherzer defocus

$\Delta f = -12$ nm; $R = 0.1$ nm

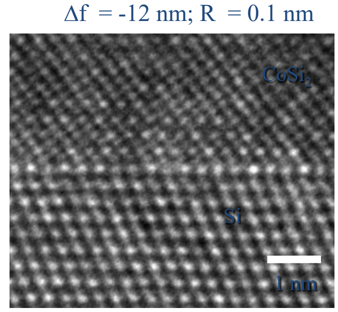

Scherzer defocus (AFI)

B. Kabius, S. Mantl
Argonne, Juelich: ~1997
CM200

Delocalization : $R = | C_5 \lambda^5 g^5 + C_3 \lambda^3 g^3 + \lambda C_1 g |_{max}$

94

94

C_s/C_c Aberration Corrections also further helps to minimizes delocalization

$$\Delta R_{coe} = \lambda g(C_1 + C_c\Delta E/E_0 + C_s(\lambda g)^2 + C_5(\lambda g)^4)$$

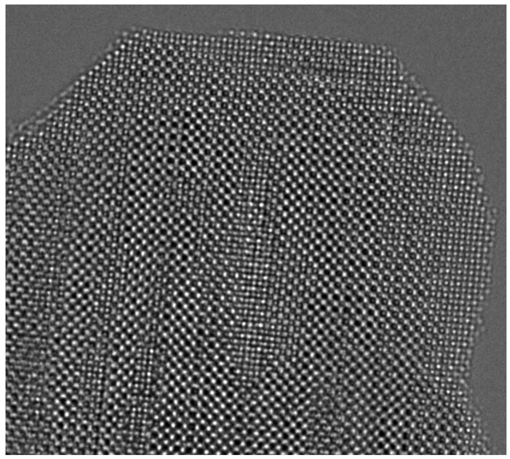

STO-LMO

95

Positive Phase Contrast Imaging

Dark
Atoms

White
Atoms

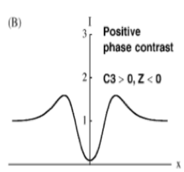

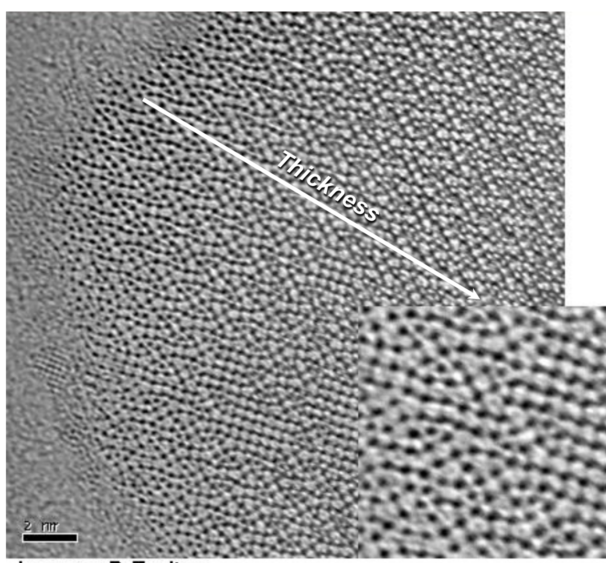

Image : B.Freitag

96

Positive Phase Contrast Imaging

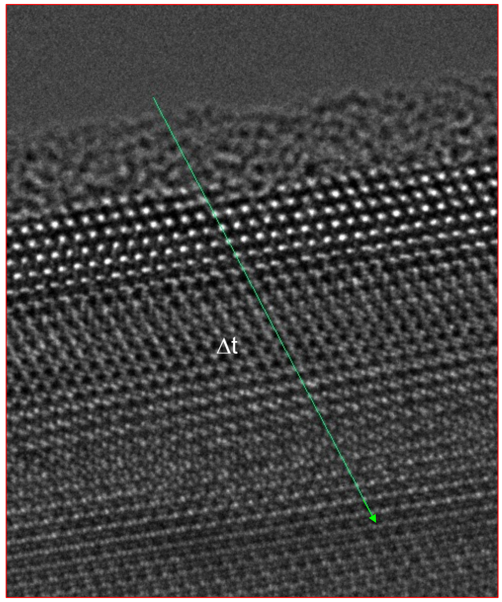

Very thin samples are not easy or common

FFT of Amorphous Carbon to adjust Stigmators

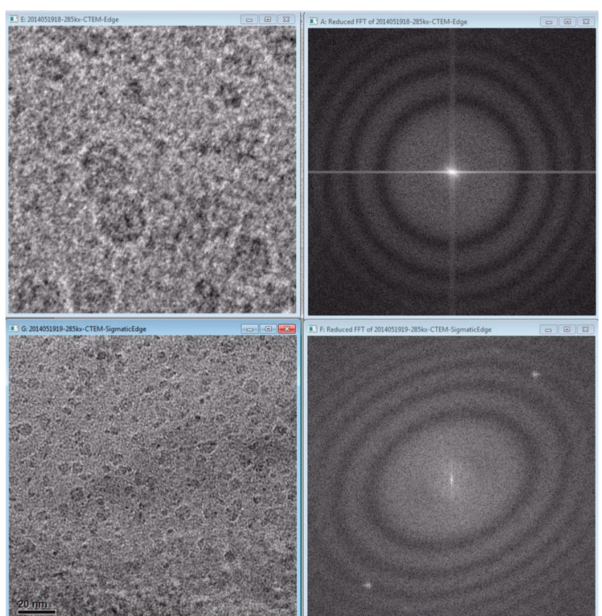

Good

Poor

Which Image is in Focus

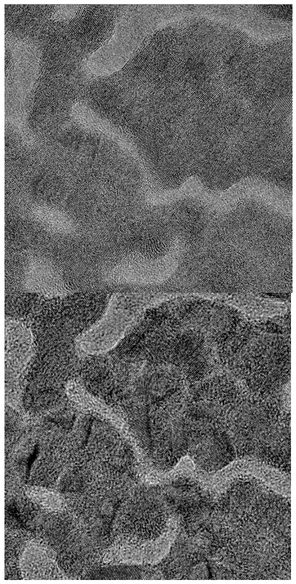

Scherzer Focus using FFT

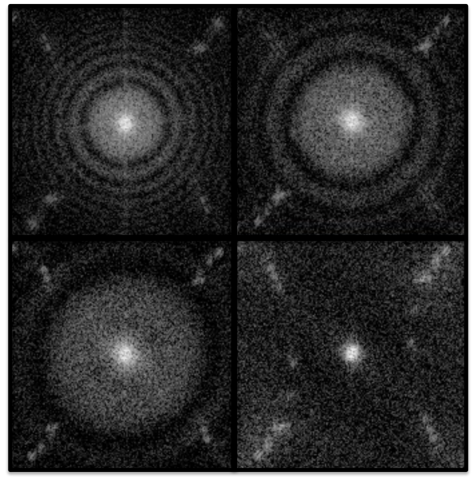

"1st Dark FFT Ring" at the Periphery of the FFT
⇒ Maximizing the information transfer

Ultra High Resolution is not "trival" even with a Corrector

Sample must be very thin and the alignments both
of the instrument and the specimen excellent

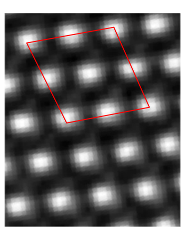

Thick & Just out
of Alignment

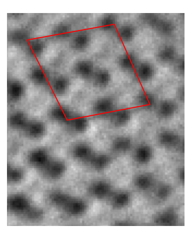

Thin &
Aligned
(but not perfectly)

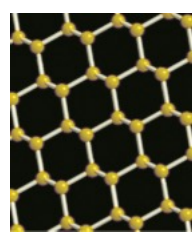

Si
{110}

….. and for UHREM direct structural correspondence
is not common ⇒you should expect to do an image simulation/calculation !!!

Direct structural interpretation of phase contrast imaging is most cases elusive.

Iterative image simulation is almost always required.

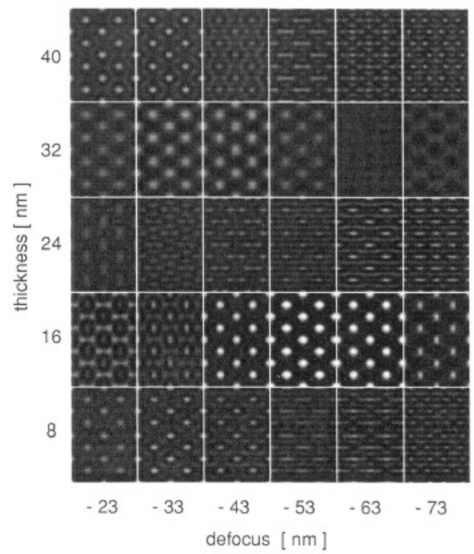

Fig. 15. A defocus - thickness map of the Fe_3Al intermetallics

HREM Image Simulation

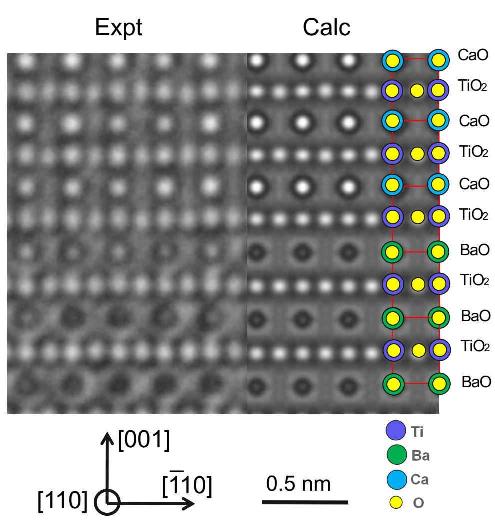

HREM image simulation using JEMS with multislice method. Major simulation parameters are: Cs: 3 μm, C5: -1.79 mm, Cc = 1 μm. Thickness: 10 nm, defocus: 3nm. Energy spread: 0.8 eV.

The Ba/O columns show dark contrast in the middle surrounded by white ring, while the Ca/O columns are opposite. Note the Ba/O or Ca/O columns at interface show different contrast as inside sublayer due to the mixture of Ba and Ca.

JG Wen ANL Electron Microscopy Center

Negative Cs Imaging – NCSI

White (Bright) ATOMS

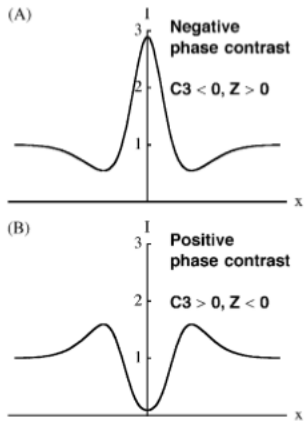

Figure 6. Intensity distribution at a single atom column with bright-atom and dark-atom contrast. **A:** Imaging with small negative spherical aberration, C_3, combined with a small overfocus, Z, provides negative phase contrast. **B:** Imaging with a small positive spherical aberration, C_3, combined with a small underfocus, Z, provides positive phase contrast.

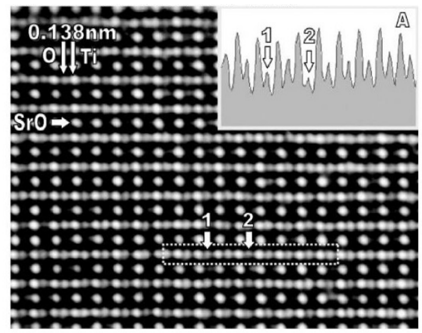

Figure 3.3 Experimental image of $SrTiO_3$ taken along the [110] zone axis employing the NCSI technique (FEI Titan 80–300 with imaging corrector, operated at 300 keV). All three atomic species are visible (compare inset) at bright contrast on a dark background.

C_3 ~ - 40 μm, df ~ + 10 nm @ 200 kV

Chun-Lin Jia, Markus Lentzen,* and Knut Urban

Microsc. Microanal. 10, 174–184, 2004
DOI: 10.1017/S1431927604040425

103

NCSI Direct Structural Mapping is interpretable only when t < ~ 6nm

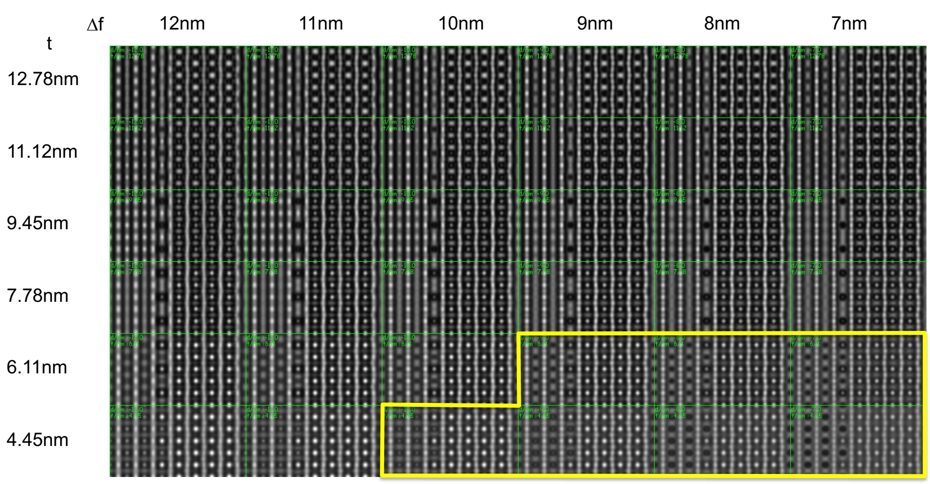

C_3 = - 40 μm, C_c = 1.5 mm

Yellow zone outlines conditions for DSM

Very little to no atomic number contrast

104

There are other contrast mechanisms in your “tool box”

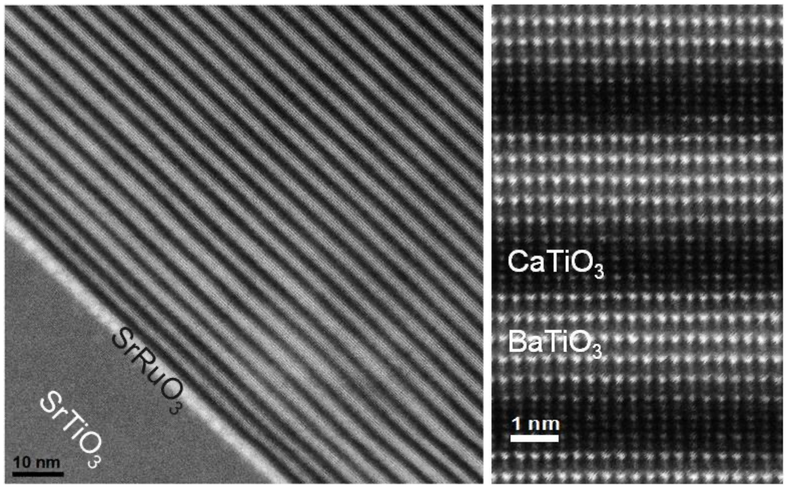

STEM – HAADF Images
can also include “Z-contrast”

Amplitude Contrast Imaging Technique Sensitive to Channeling

Channeling Theory

When crystal is aligned along zone axis, the interaction of electrons with an atom column is very strong. Due to the strong electrostatic potential of the atoms , an atom column acts as a channel for the incoming electrons. By passing through successive atoms, the electron wave oscillates along channeling direction as shown below. This oscillation length, called extinction distance, is a function of the average mass density of the column, depending on chemical composition and zone axis.

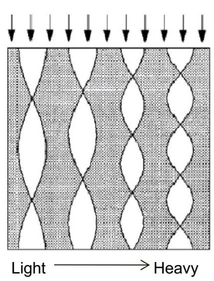

Schematic diagram of electron channeling

extinction distance

$$D_{1S} = \alpha\left[\frac{d^2}{Z} + 0.276B\right].$$

α, a constant
d, distance between successive atoms along column
Z, atomic number
B, Debye-Waller factor

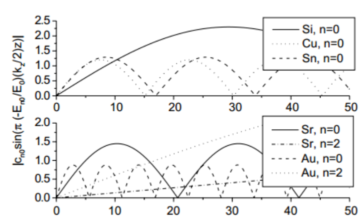

Example s of extinction distances

As shown in the right figure, different atoms have different extinction distance. The intensity of atom columns oscillates depending on thickness. Defocus can change the phase of the oscillation.

A. Wang, F.R. Chen, S. Van Aert, D. Van Dyck, **Ultramicroscopy**, 110 (2010) 527.

Beyond NCSI- With access to C_c we can use the Aberration Coefficients as adjustable parameters to adjust/optimize imaging conditions –

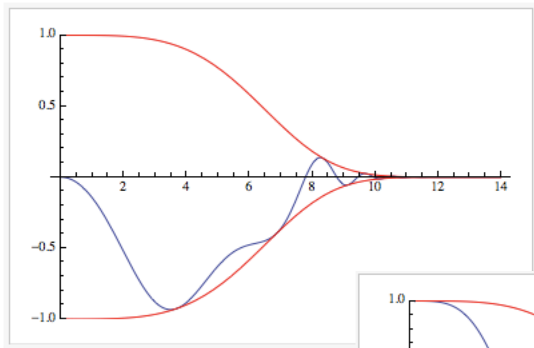

$C_1 = \delta f$
$C_3 \sim 0.1$ mm
$C_c \sim 1.5$ mm
$C_5 \sim -2$ mm

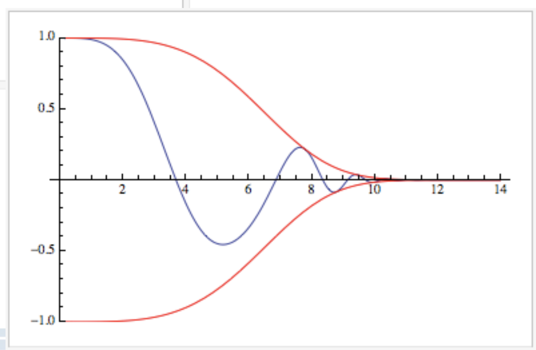

107

Tuning $C_1/C_3/C_c$

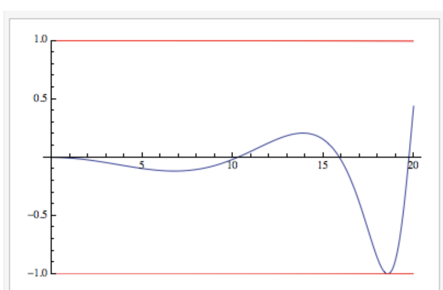

$C_1 = \delta f$
$C_3 \sim 3$ μm
$C_c \sim 10$ μm
$C_5 \sim -2$ mm

Amplitude Contrast Imaging (ACI)

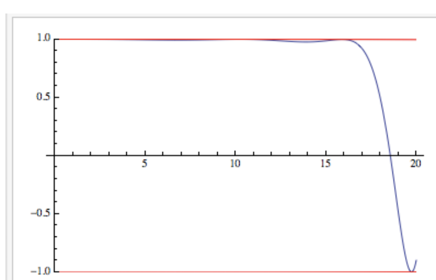

108

ACI – Imaging of Ferroelectric 4x4 Superlattice - $CaTiO_3$ / $BaTiO_3$

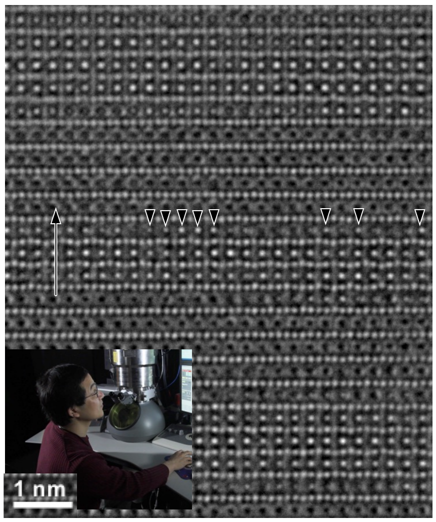

[110]

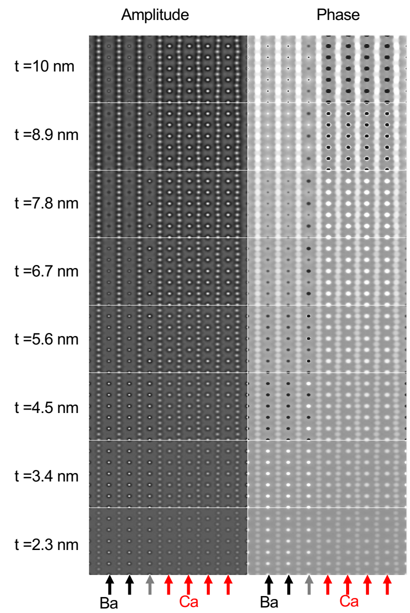

JG Wen – ANL Electron Microscopy Center

TEM vs STEM

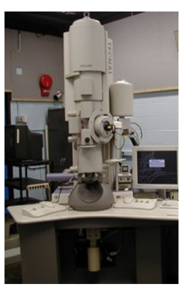

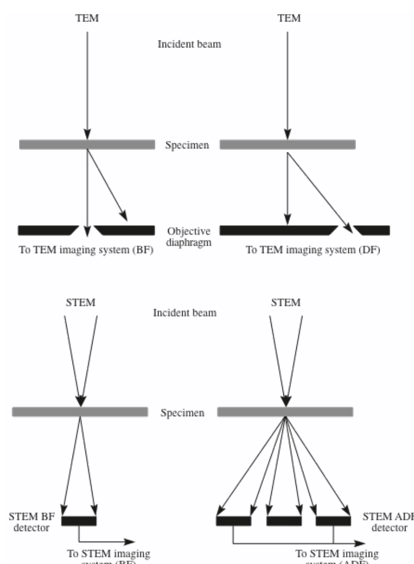

Why Bother??